Breaking of axial symmetry in excited heavy nuclei as identified in GDR data

Grosse, E.; Junghans, A. R.; Massarczyk, R.;

Originally published:

November 2017

European Physical Journal A 53(2017), 225

DOI: https://doi.org/10.1140/epja/i2017-12415-2

Breaking of axial symmetry in excited heavy nuclei as identified in GDR data

E. Grosse,[1,*] A.R. Junghans,[2,†] and R. Massarczyk[1,2,‡]

[1] *Institute of Nuclear and Particle Physics, Technische Universität Dresden, 01062 Dresden, Germany*
[2] *Institute of Radiation Physics, Helmholtz-Zentrum Dresden-Rossendorf, 01314 Dresden, Germany*

A recent theoretical prediction of a breaking of axial symmetry in quasi all heavy nuclei is confronted to a new critical analysis of photon strength functions of nuclei in the valley of stability. For the photon strength in the isovector giant dipole resonance (IVGDR) regime a parameterization of GDR shapes by the sum of three Lorentzians (TLO) is extrapolated to energies below and above the IVGDR. The impact of non-GDR modes adding to the low energy slope of photon strength is discussed including recent data on photon scattering and other radiative processes. These are shown to be concentrated in energy regions where various model calculations predict intermediate collective strength; thus they are obviously separate from the IVGDR tail. The triple Lorentzian (TLO) ansatz for giant dipole resonances is normalized in accordance to the dipole sum rule. The nuclear droplet model with surface dissipation accounts well for positions and widths without local, nuclide specific, parameters. Very few and only global parameters are needed when a breaking of axial symmetry already in the valley of stability is admitted; a reliable prediction for electric dipole strength functions also outside of it is expected.

I. INTRODUCTION

The ongoing discussion [1–4] about triaxial shapes in heavy nuclei, recently often studied off stability, may provoke the question, how well the widely used assumption about axial symmetry of most less exotic nuclei is founded on sufficiently sensitive experimental data. Actually, a recent theoretical prediction [5] (constrained HFB calculations with the Gogny D1S interaction) as tabulated for a large number of nuclei indicates broken axial symmetry for quasi all of them. A nonaxial shape of heavy nuclei is a less stringent assumption than the often made assumption of axiality, which probably originates from atomic hyperfine structure observations [6], which are usually made on unpolarized samples and thus are insensitive to broken axiality. In formal logics it was formulated nearly 100 years ago by K. Popper: "Any theory in the empirical sciences can never be proven by observations, but it can be falsified". Hence a support for the predicted non-axiality has to rely on a falsification of the prejudice of an axial or even spherical shape for most heavy nuclei. This does not exclude the possibility, that certain properties as observed in certain nuclei may be reproduced well by a theoretical model based on such a symmetry.

Subsequent to a more formal discussion of the influence of nuclear shapes on photon interactions we will present in this paper how breaking axial symmetry influences the splitting of the IVGDR. In text books this feature is often considered an indicator of nuclear deformation, and our detailed investigation aims for facts conflicting an assumption of axiality. Such features will be regarded for more than 20 nuclei (as examples) in a wide range of mass number A and ground state quadrupole moments, *i.e.* deformation. As an introduction to the question of nuclear shape symmetry, information from low energy nuclear structure studies in support of triaxiality will be presented first. Detailed Coulomb excitation studies will be surveyed, as they are more sensitive to the breaking of nuclear shape symmetries [7, 8] than the observation of energy spectra, which have been interpreted in the past preferentially assuming *ad hoc* axial symmetry of nuclei in the valley of stability [9–12]. To properly define parameters we will first quantify the connection of nuclear shapes to electric quadrupole moments and transition rates, which are both considered an experimental information on these.

After a short discussion of the fundamental origin [13] of the sum rule for the electromagnetic strength in nuclei, a parameterization of the IVGDR as seen in photonuclear reactions with heavy nuclei will be presented. In contrast to previous work the electric dipole strength is derived from IVGDR data without assuming axial symmetry as it was usually made for most heavy nuclei; instead theoretical [5] deformation and triaxiality parameters will be used. As was noted recently for nuclei with mass number $A > 70$ [14], the apparent width of the IVGDR is an important parameter in the characterization of especially its low energy tail. We will thus critically regard predictions made in the past on the energy-dependence of this width and its eventual relation to the deformation induced split. Interesting insight is gained by a close look on various experimental data on photon emission and absorption for this tail region; here intermediate structure has been observed since long [15, 16]. This information on minor strength in the tail region, nowadays usually related to 'pygmy' and other modes [17–20], will be discussed in view of multipolarity and the possible influence on an extrapolation to energies of relevance for predictions on neutron capture. In sections IV and VI energy

* electronic address: e.grosse@tu-dresden.de
† electronic address: a.junghans@hzdr.de
‡ present address: Los Alamos National Laboratory, Los Alamos, New Mexico 87545, USA

dependent dipole strength functions resulting from the combination of IVGDR and minor strength will be presented for nuclei in a wide range of even and odd A. As the respective experimental studies can often only be performed for nuclei in or close to the valley of beta-stability, we aim for a small number of global parameters to increase the reliability of any extrapolation.

II. NUCLEAR DEFORMATION AND QUADRUPOLE DATA

Quadrupole moments

The electromagnetic response of nuclei has played an important role for the exploration of the size of nuclei and the departure of their shape from spherical symmetry was first indicated by a splitting of atomic transitions due to the nuclear electromagnetic field [6]. Much improved and accurate hyperfine structure measurements, partly using laser techniques, determined the 'spectroscopic' electric quadrupole ($\lambda = 2$) moment Q_s of the ground state [21] in nearly 800 odd nuclei. In addition, Q_s-values from the reorientation effect in Coulomb excitation as well as from muonic X-ray data became available for many even and odd nuclei. In even nuclei, Coulomb excitation-reorientation data can also yield 'spectroscopic' quadrupole moments for excited 2^+-states $Q_s(2^+)$, as compiled [21] for nearly 200 isotopes. In many cases the sizes and signs – positive and negative values are observed – of these quadrupole moments were not in agreement to predictions for single particle or hole configurations [12] and a seemingly obvious picture [9] interprets this as the result of the rotation of a non-spherical body with an 'intrinsic' quadrupole moment $Q_0 = -7/2$ $Q_s(2^+)$. If the sign of $Q_s(2^+)$ was determined, it mostly was negative indicating an oblate charge distribution in the laboratory system and an intrinsic prolate deformation. For most even nuclei away from closed shells the large Q_0 values observed were interpreted as a strong indication for a cigar like deformation, especially for lanthanide ($A \approx 170$) and actinide nuclei ($A \approx 240$). Mainly for isotopes in the near magic Os-Pt-Hg region positive $Q_s(2^+)$ were observed [8, 22], indicating oblate intrinsic shapes, *i.e.* $Q_0 < 0$. Assuming axial symmetry and a homogeneous distribution of the charge within the nuclear volume, a rotational model was formulated, in which the intrinsic electric quadrupole moment Q_0 of even nuclei is related to the radius difference ΔR between the long and the two short axes of the shape by [9]:

$$Q_0 \equiv \sqrt{\frac{9}{5\pi}} Z R^2 \beta (1 + b\beta) \qquad (1)$$
$$\beta \cong \frac{4}{3}\sqrt{\frac{\pi}{5}}\frac{\Delta R}{R} \cong 1.057\frac{\Delta R}{R}$$

The rotational model relation in Eq.(1) between deformation β, Q_0 and ΔR is widely applied when electromagnetic data are related to calculated nuclear (mass) deformations usually characterized by β. For years $b \approx 0.16$ was used [9, 23], but reference is also often made to a compilation of electric quadrupole transition widths [24], which proposed $b = 0$ as approximation.

Axiality and observations

The energies and angular momenta of the levels in heavy nuclei have been regarded [9, 16, 24] in view of single particle as well as collective excitations like rotations or vibrations of the nuclear body as a whole. The model of a rotating axially symmetric liquid drop with a quadrupole moment, representing an even nucleus, predicts one 2^+-state with a "collective" *i.e.* enhanced E2-transition width. In this model the intrinsic structure for the ground state 0^+ and the lowest 2^+-state r are assumed to be the same. Then the reduced matrix element (in e fm^2) of the electric quadrupole transition E_γ (in MeV) of this 'rotational' state r to ground is related [9, 12] to Q_0 (in fm^2) by:

$$|\langle r\|\mathbf{E}2\|0\rangle|^2 = \mathrm{B(E2}, 0 \rightarrow r) = \frac{5}{16\pi}Q_0^2 \qquad (2)$$

The E2 ground state decay width $\Gamma_{r0}(E_\gamma)$ (in MeV) is obtained from the relation (valid in general):

$$\Gamma_{r0}(E_\gamma; \mathrm{E2}) = \frac{4\pi}{75}\frac{\alpha E_\gamma^5}{g(\hbar c)^4}|\langle r\|\mathbf{E}2\|0\rangle|^2 \qquad (3)$$
$$g = \frac{2J_r + 1}{2J_0 + 1}$$

where $\alpha, \hbar$ and c are the fine structure constant, the reduced Planck constant and the velocity of light; J_0 and J_r are the spins of the ground state and the excited level. The Q_0 and B(E2) are observables, and we will use Q_0 to express a deviation from sphericity in Figs. 1 and 2, where it is experimentally determined. The deformation β is a model parameter with ambiguities in its definition and we use it as defined in the calculations [5] we relate to.

One serious shortcoming of the axial rigid rotor model is the fact, that it only predicts one 'collective' 2^+-state. Experimentally at least two 2^+-levels with enhanced transitions to the ground state are observed in nearly all even nuclei. This has led to the assumption [12, 23] that a semiclassical coupling of the collective rotation to a collective quadrupolar vibration around a deformed basis state can be used to get deformation parameters β and γ from a fit to experimental data. Instead we refer to a microscopic calculation in a self-consistent scheme [5], results of which are available for practically all heavy even nuclei between the neutron and proton drip lines. In Fig. 1 the correlation between γ and Q_0 is depicted for nuclei in the valley of stability as it results from this CHFB-calculation. This work only assumes R_π-invariance, *i.e.*wave functions stay unchanged after

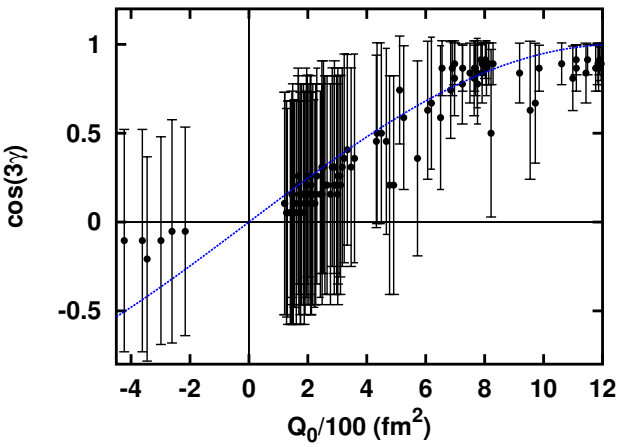

FIG. 1. (Color online) Correlation between $\cos(3\gamma)$ and Q_0 in ≈ 170 even nuclei with $60 < A < 240$; the respective data are taken from a CHFB+GCM calculation [5] for nuclei in the valley of stability and correspond to its minimum and to nuclei between two less and two more neutrons. The bar lengths represent the standard deviations in γ as given by these calculations and tabulated as supplemental material; the dashed blue curve serves as eye guide to compare the trend of the calculations to experimental data as presented in Fig. 2, where it is depicted as well.

a rotation by 180 degree. It finds non-zero expectation values for triaxiality $\langle\gamma\rangle \neq 0$ in nearly all heavy nuclei, and in some cases the predicted standard deviation does not include $\gamma = 0$, what corresponds to $\cos(3\gamma) = 1$. In Fig. 1 the density of symbols is of significance, as all the nuclei from a small band near beta-stability are depicted. The clear clustering at $Q_0 \approx 200\text{fm}^2$ and $\cos(3\gamma) \approx 0.2$ will play an important role for the discussion of IVGDR data in these numerous nuclei, previously often regarded transitional between axial and spherical in shape.

The CHFB calculations used here "are free of parameters beyond those contained in the Gogny D1S interaction" (adjusted to the properties of nuclei with small Q_0) and based on "a density-dependent HFB approximation. They describe simultaneously the gross properties depending on the average field as well as the effects of pairing correlations via the Bogolyubov field with the same force" [25]). The use of constrained wave functions and the approximate projection on good angular momentum by the generator coordinate method are especially important at low angular momentum and the calculations generate at least two 'collective' 2^+-levels in nearly all nuclei. Results on triaxiality obtained in Hartree-Fock-Bogolyubov (HFB) calculations for the intrinsic system are subject to significant change when the order of variation and projection on angular momentum in the observer's frame are interchanged [5, 26]. Long ago it was pointed out [27], that the quantum mechanically proper variation after projection may shift the γ-oscillation centered at axiality to $\langle\gamma\rangle \neq 0$. One way to circumvene this problem is to parameterize the quadrupole degrees of freedom as seen by the observer in the laboratory, as is done implicitly by a interacting boson approximation (IBA) [28–30]. A rather convincing agreement to E2-transition data as well as level energies is achieved by this group theoretical ansatz, when adjusting parameters for a given region of the nuclide chart and then comparing experiments to the predictions for other nuclei in that region. A global description of all heavy nuclei was not reached yet, but by a distinction between neutron and proton 'Bosonic' modes a hint for nonaxiality was found (IBA-2) [31]; an inclusion of Giant Resonance modes would be of great interest. Another way to avoid the problems related to the necessary projection into the observer's frame is the construction of rotational invariants from experimentally observed transition rates [7]. Data from of heavy ion induced multiple Coulomb excitation of low lying levels in heavy nuclei were analyzed on the basis of such invariants [8, 32] and for many heavy nuclei the breaking of axial symmetry was indicated by these experimental data. This analysis excels an older, comparatively simple, model of a rigid triaxial rotor [33] which directly delivers two collective 2^+-levels. Generalizing Eq. (2) Q_0 is replaced by an intrinsic Q_i defined by the sum of several (in the case of a rigid triaxial rotor 2) squared E2-matrix elements:

$$Q_i^2 \equiv \frac{16\pi}{5} \sum_{r=1,s} |\langle r\|\mathbf{E2}\|0\rangle|^2 \qquad (4)$$

Experimental data [34] show that a limitation to one term in the sum ($s = 1$) leads to an error of less than 10% in Q_i and thus for the figures it suffices to use Eq. (2) instead of Eq. (4) to depict Q derived from B(E2)-values. In the rotation invariant ansatz [7] the deviation from axial symmetry is described by the parameter $\cos(3\gamma)$, which in principle can be directly derived from transition rates observable in multiple Coulomb excitation [2, 8, 35–37]. In quantal systems like nuclei only expectation values are accessible to measurements; Q_0 and $\cos(3\gamma)$ in Figs.(1, 2) are to be understood as symbols for the actually determined quantities; explicitely these are $\langle Q_i^2\rangle$ and $\langle Q_i^3 \cos(3\gamma)\rangle$. In various nuclei the inclusion of triaxiality produced transition rates close to data [37–39], especially when surface vibrations are included as a perturbation. But in most heavy even nuclei more than 2 collective 2^+-levels are observed and this scheme has to be generalized further. Employing tensor algebra and assuming reflection symmetry as well as identical distributions of protons and neutrons Eq. (4) was shown [7, 8, 37] to be valid also for heavy nuclei in general, as long as the sum includes all relevant 2^+-strength, especially all collective 2^+-levels. Then Eq.(4) with $s > 2$ represents an unweighted sum rule which is rotation invariant and thus valid in the laboratory as well as in the intrinsic frame.

In Fig. 2 the correlation of the parameters Q_0 and $\cos(3\gamma)$ is displayed for more than 150 nuclei, for which relevant data have been published [2, 8, 22, 29, 32, 35–37, 40–42]. The rather complex experimental investiga-

tions on triaxiality were performed for a limited number of nuclei only, but a comparison to the prediction [5] shown in Fig. 1 indicates a clear trend to triaxiality with decreasing Q_0. Here ($cos(3\gamma) \to 0$), whereas most well deformed nuclei and especially the actinides show smaller deviations from axiality. The small number of nuclei which are oblate with ($\cos(3\gamma) < 0$) already at low E_x does not allow similar conclusions, and for very small Q_0 the split of the IVGDR is so small, that nonaxiality is not observable there.

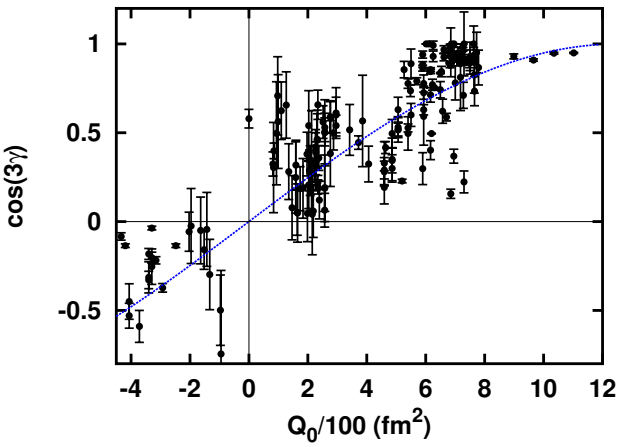

FIG. 2. (Color online) Correlation between $\cos(3\gamma)$ and Q_0 in $\approx$ 150 even nuclei with $A > 60$, for which respective experimental data are available. The bars correspond to experimental uncertainties and the dashed blue curve serves as eye guide to compare the trend of the data to the one of the calculations as presented in Fig. 1, where it is depicted as well.

If not determined directly, the sign of Q_0 was assumed to coincide with the one of $\cos(3\gamma)$; unambiguously opposite signs for these two quantities were not reported yet. Data for odd nuclei [43] are omitted in the Figure, we only state that they support the findings presented here. Also not given in the Figure are variances that can be derived in principle from an extension of the above formulae [2, 7, 8, 37], but the experimental uncertainties of respective data do allow a rough extraction of such information only. The experimental data show a very similar trend of the axiality increasing with Q_0 as seen in the calculation. The trend as indicated as blue dashed curve in figs. 1 and 2 suggests an approximate representation of nuclear shapes by one parameter Q_0 only, with the axiality depending on it. The split of the giant dipole resonances [11] is related to the axis lengths $R_{1,2,3}$. Assuming R_π-invariance only, the combination of Eq. (13) to Eqs.(19-21) of ref. [7] results in relations for the three axes R_i of the ellipsoid in the body-fixed system as derived from its shape parameters:

$$\begin{aligned} 5Q_i\cos(\gamma) &= Z(2R_3^2 - R_1^2 - R_2^2) \\ 5Q_i\sin(\gamma) &= \sqrt{3}Z(R_1^2 - R_2^2) \\ R_0^3 &= R_1R_2R_3 \end{aligned} \tag{5}$$

The last line uses the concept of the conservation of the nuclear density in an equivalent ellipsoid, which has the same volume $V = 4/3\pi R_0^3$, and the three harmonic oscillator constants ω_k are inversely proportional to R_i. Assuming the same charge Ze for the ellipsoid as for the non-spherical nucleus, Eq. (5) can be related directly to the information about R_0, the quadrupole moment Q_i and the triaxiality γ of that nucleus. The similarity between observations and the CHFB-calculations [5], as shown in Figs. 1 and 2, suggests to use these as a reference. The equivalent sphere radius $R_0 = \sqrt{(5/3)}\langle R_p\rangle$, with the tabulated [5] point proton radius R_p, will also enter into the predictions discussed below. The tabulated β and γ values are related to the oscillator parameter ratios P_{CHFB} and Q_{CHFB}, the direct outcome of these calculations [5] (with Q_{CHFB} not equivalent to a quadrupole moment). These are used in Eq. (6) as axis ratios to obtain the radii R_i from R_0:

$$\begin{aligned} R_1 &= R_0 \cdot (P_{CHFB}Q_{CHFB})^{-1/3} \\ R_2 &= P_{CHFB} \cdot R_1 \\ R_3 &= Q_{CHFB} \cdot R_1 \end{aligned} \tag{6}$$

with

$$\begin{aligned} x &= \frac{\beta}{2\beta+1} \\ P_{CHFB} &= \exp\left(-x\sqrt{3}\sin\gamma\right) \\ Q_{CHFB} &= \exp\left(x\left[\frac{3}{2}\cos\gamma - \frac{\sqrt{3}}{2}\sin\gamma\right]\right) \end{aligned}$$

In ref. [5] supplemental material is given for 1712 even-even nuclei including their deformation parameters, from which the corresponding 'triaxial oscillator parameters' can be derived, which are inversely proportional to the axis lengths. The extraction of these axis ratios differs formally from Eq. (5) as well as from the Hill-Wheeler [44] formula used by us before [14]. It can easily been shown numerically, that for the small Q_i in the range of interest the differences are below 25% and hence not significant. For the calculation of fission barrier heights more exact prescriptions may be needed, but, as was pointed out already long ago [45, 46], the consideration of broken axiality is even more important in that case.

III. PHOTON ABSORPTION BY NUCLEI

The non-resonant interaction between photons and objects of charge Ze and mass M is quantified by the Thomson scattering cross section $8\pi(Z^2\alpha\hbar c)^2/3(Mc^2)^2$ with α

denoting the fine structure constant, c the velocity of light and $\hbar$ the Planck constant divided by 2π; for ^{208}Pb it amounts to 0.02 fm^2 only. In addition to this direct process a photon of sufficiently high energy E_γ excites nuclei from the ground state resonantly; this is described by a Lorentzian centered at the resonance at E_r with total width Γ_r:

$$\sigma_\gamma \cong I_{r0}\frac{2}{\pi}\frac{E_\gamma^2\Gamma_r}{(E_r^2-E_\gamma^2)^2+E_\gamma^2\Gamma_r^2} \tag{7}$$

The integral of the absorption cross section σ_γ over the resonance, which has spin J_r is denoted by I_{r0}:

$$I_{r0}=\int\sigma_\gamma(E_\gamma)dE_\gamma=\frac{g(\pi\hbar c)^2\Gamma_{r0}}{E_r^2};\quad g=\frac{2J_r+1}{2J_0+1} \tag{8}$$

where Γ_{r0} is the partial width of the transition between the resonant level (E_r, J_r) and the nuclear ground state $(0, J_0)$. As described by Eq. (3) for E2-excitations, it is directly proportional to the square of the electromagnetic transition matrix element; a respective relation exists for electric and magnetic excitation with multipole order $\lambda = 1$:

$$\Gamma_{r0}(E_\gamma;E,M1)=\frac{16\pi}{9}\frac{\alpha E_\gamma^3}{g(\hbar c)^2}|\langle r\|\mathbf{E},\mathbf{M}1\|0\rangle|^2 \tag{9}$$

Derived from very general conditions as causality and analyticity together with dispersion relations from QED the interaction of short wavelength photons with nuclei of mass number $A = Z + N$ can be 'integrated up to the meson threshold' analytically, leading to the energy-weighted sum rule of Gell-Mann, Goldberger and Thirring (GGT) [13]:

$$\begin{aligned} I_{\rm A} &= \int_0^{m_\pi c^2}\sigma_\gamma(E_\gamma)dE_\gamma \\ &\cong 2\pi^2\frac{\alpha\hbar^2}{m_n}\left[\frac{ZN}{A}+\frac{A}{10}\right] \\ &\cong 5.97\left[\frac{ZN}{A}+\frac{A}{10}\right]\,\text{MeVfm}^2 \end{aligned} \tag{10}$$

Here m_n and m_π stand for the mass of nucleon and pion, respectively and no arguments [47] about the nuclear absorption of photons with energies above $m_\pi c^2$ are needed. The second term "contains all of the mesonic effects" and is assumed [48] to be accurate within 30%. It was approximated by assuming "that a photon of extremely large energy interacts with the nucleus as a system of free nucleons", and a correlation to hadronic shadowing was investigated to be weak [48]. Eq. (10) includes all multipole modes of photon absorption and the first term in the sum is identical to the "classical (TRK) sum rule" for electric dipole radiation [49] as the contribution to other multipoles will be shown to be small. Absorption by the nucleons does not contribute below $E_\gamma = m_\pi c^2$, but nucleon pairs and especially p-n-pairs are strongly dissociated by photons with $20 < E_\gamma < 200$ MeV. The respective "quasi-deuteron effect" has been derived from the expression valid for the free deuteron by correcting for Pauli blocking [50].

The photo-disintegration of nuclei is one of the nuclear reactions studied the earliest. Soon after it's discovery it has been recognized as dominating photon absorption by an excitation of the IVGDR. This isovector nuclear electric dipole resonance represents a strongly collective oscillation of neutrons against protons. The good agreement in the region below 20 MeV seen in Fig. 3 indicates that the first term in Eq. (10), a Lorentzian in accordance to the classical electric dipole sum rule (TRK, [49]) is a good ansatz to describe the IVGDR. Photo-neutron data are available [51] for ^{208}Pb up to energies above $m_\pi c^2$ as shown in Fig. 3.

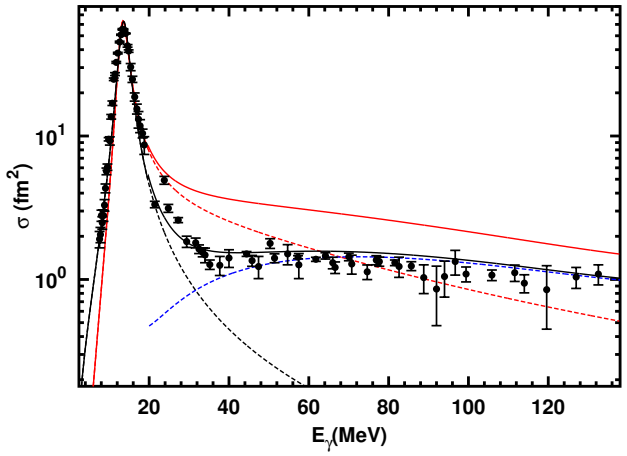

FIG. 3. (Color online)Cross section of photo-neutron production data [51] on ^{208}Pb in comparison to a Lorentzian for the isovector IVGDR (black and red lines, see text) and the quasi-deuteron effect (blue dashed line). The sum of both contributions is given as drawn lines. In ^{208}Pb a deformation induced widening can be neglected as will become obvious in Fig. 18.

They are compared on an absolute scale to a Lorentzian like in Eq. (7) with pole energy $E_r = 13.6$ MeV and I_r normalized such that it's integral agrees to the first term in Eq. (10), the expression for the absorption corresponding to the quasi-deuteron mode[50] for $E_\gamma > 20$MeV. The sum of both is depicted as well and the case of a constant width $\Gamma_r = 3.0$ MeV is shown in black. In red the change is demonstated which evolves from making the width proportional to the square of the photon energy $\Gamma_r \sim (\frac{E_\gamma}{E_r})^2$. The latter proportionality was proposed [52] to evolve from Landau theory of Fermi liquids. Obviously the data above 25 MeV are clearly below the curve corresponding to an IVGDR-Lorentzian with an increasing width. The cross section is well reproduced on absolute scale without such a change and its integral agrees to the second term in Eq. (10); it is worth

mentioning that a similarly situation was published [50] for other nuclei. The cross section observed to exceed the sum between 20 and 30 MeV may be identified with the contribution from the IVGQR as shown in section VI. In contrast to elastic electron scattering [53, 54] the cross section depicted in Fig. 3 shows only weak signs of giant resonances of multipolarity other than E1. The disagreement especially in the high energy slope as seen in Fig. 3 and also Fig. 4 is obvious when a proportionality between width and photon-energy squared is imposed; hence the KMF-theory [52] is falsified at least for ^{208}Pb.

The KMF-model was allegedly derived from the theory for Fermi liquids although a detailed relation to the work of Landau or Migdal is not given in that work [52], which explicitly states below its Eq. (29), that a "direct comparison" between the "spreading width" in a Lorentzian for the GDR and the one of the theory of Fermi liquids is "difficult... and not clear" [52], and they further assume *ad hoc* without any additional arguments, that they coincide. The KMF-model was favoured within the Reference Input Parameter Library (RIPL) project [55] to improve the agreement to some data below the IVGDR. But at variance to the original paper [55], a more recent work [56] from that collaboration now proposes to insert a linear decrease of Γ_r with E_γ into Eq. (7) instead of a quadratic one. Also work published some time ago was not in favour of the KMF-model: (1) Fundamental theoretical arguments have been used to show, that "Landau damping is not the appropriate process for describing the damping of the low-multipole giant resonances" [57]. (2) It was demonstrated [58] for the nucleus ^{163}Dy that the KMF-model does not work, when 2-step cascade data are analyzed using a double Lorentzian for the IVGDR; also for ^{157}Gd (see Fig.fig. 13) this model wasnot favoured by authors ([59], who had first proposed its use earlier.

Although the IVGQR is not a distinct quantum level, but a sum of densely packed levels resonantly enhanced, it can be described by a sum of Lorentzians [60]. The possibility of a Lorentzian was tested numerically at hand of data for a few nuclei [61]. Derived from Eq. (7), but now applied to a wide giant 'collective mode' forming an envelope over narrow electric dipole states excited by E1 radiation, Eq. (11) will be used for the parameterization of the IVGDR, with k characterizing a deformation induced split. For the sum of k Lorentzians, the main term of Eq. (10), the classical sum rule for E1, is divided equally into k fractions, assuring a normalization of the integrated strength:

$$\frac{dI_{\rm E1}}{dE_\gamma}(E_\gamma) \equiv \sigma_{abs}^{\rm E1,IV}(E_\gamma) \cong 5.97\frac{ZN}{A}\frac{2}{k\pi}\sum_{i=1,k}\frac{E_\gamma^2\Gamma_i}{(E_i^2-E_\gamma^2)^2+E_\gamma^2\Gamma_i^2}{\rm fm}^2 \quad (11)$$

In Fig. 3, asssuming ^{208}Pb to be spherical even above 10 MeV, $k = 1$ was used. It will be shown in sections IV and VI, that the TRK sum rule can be well fulfilled for all heavy nuclei, when account is made for the breaking of axial symmetry leading to $k = 3$. As long as the sum rule is respected, the extraction of dipole strength in the region of the maximum and of the height of the low energy tail are fixed unambigously by the use of radii, deformation and triaxiality from the CHFB calculations [5]. Using Eq. (6), the energies of the three resonance poles are derived from the spherical centroid energy $E_0 = E_{IVGDR}$ and the well known proportionality between E_i and $1/R_i$. For E_0 of Eq. (12) we note that two historic theoretical treatments of the IVGDR predict its energy rather well for medium mass nuclei [62], respectively for the very heavy ones [63]. By using concepts of the droplet model these two approaches were unified [64]. The symmetry energy $J = 32.7$ MeV and surface stiffness $Q = 29.2$ MeV are taken from the finite range droplet model [65] and the IVGDR centroid energies $E_0(Z, A)$ will be shown for $78 < A < 254$ to be well predicted with only one additional quantity, an effective nucleon mass. It was adjusted in an overall fit to the IVGDR positions and we obtained $m_{eff} = 800{\rm MeV}/c^2$, which differs from our earlier work [14] where $874{\rm MeV}/c^2$ was used. This change is due to the different choice of the nuclear radius as $R_0 = \sqrt{(5/3)}\cdot\langle R_p\rangle$ with the point proton radius $\langle R_p\rangle$ taken from the CHFB calculations [5]. Hence only very few parameters for the centroid energy of the IVGDR's are required in a global desccription. As previously [14, 66] we follow [64] and use (with units MeV and fm):

$$E_0 = \frac{\hbar c}{R_0}\sqrt{\frac{8J}{m_{eff}}\cdot\frac{A^2}{4NZ}}\left[1+u-\varepsilon\cdot\frac{1+\varepsilon+3u}{1+\varepsilon+u}\right]^{-1/2}$$
$$\varepsilon = 0.0768, u = (1-\varepsilon)\cdot A^{-1/3}\cdot\frac{3J}{Q} \quad (12)$$
$$E_i = \frac{R_0}{R_i}\cdot E_0 \quad \text{and} \quad \Gamma_i = c_w E_i^{1.6}$$

The nature of the IVGDR does not allow for the direct determination of its Lorentz widths Γ_i in analogy to Eq. (9), but it was predicted theoretically [67] to be related to nucleon dissipation in nuclei. Hydro-dynamical considerations [68] predict the dependence of the damping width Γ_i on its pole energy E_i to be proportional to $E_i^{1.6}$; this exponent lies between theoretical values [57] for one- and two-body dissipation. Including all the nuclides treated in this work and the axis ratios available from the CHFB calculations we obtain $c_w = 0.045(3)$. Of course, the proportionality constant c_w has an uncertainty and its uncertainty enters in the radiative width nearly linearly as the slope of a Lorentzian sufficiently far away from E_0 is quasi proportional to Γ_i. In our earlier work, a value of $c_w = 0.05$ had been used [14, 66]; there single Lorentzians were adjusted to IVGDR data for ^{88}Sr and ^{208}Pb, assumed to have one pole only. The new values for m_{eff} and c_w given now are based on the CHFB calculations [5, 69]. With one parameter for the energies and one for the widths, both adjusted to be equal for all

heavy nuclei with $A > 78$ [14, 70] one gets a good agreement to measured resonance shapes, as will be shown in Figs. 5 to 24.

We stress here a point presented above and also already in previous work [14]: the width Γ_i is varying with E_i and not with E_γ as often assumed [55, 56] by local fits to the apparent widths seen in photo-neutron data (using $k = 1$ or 2 in Eq. (11). An energy-independent width is also used in a comparison of a Lorentzian to a detailed shell model calculation [71, 72] for the nucleus ^{208}Pb, which is based on a large number of configurations. It is depicted in Fig. 4 and the width predicted as given in Eq. (12) was used. It should be noted here, that this prediction, like TLO, is normalized to the "classical" sum rule, the main component in Eq. (10). A shape induced splitting, as willl be regarded in the next section, can be assumed to be very small for ^{208}Pb.

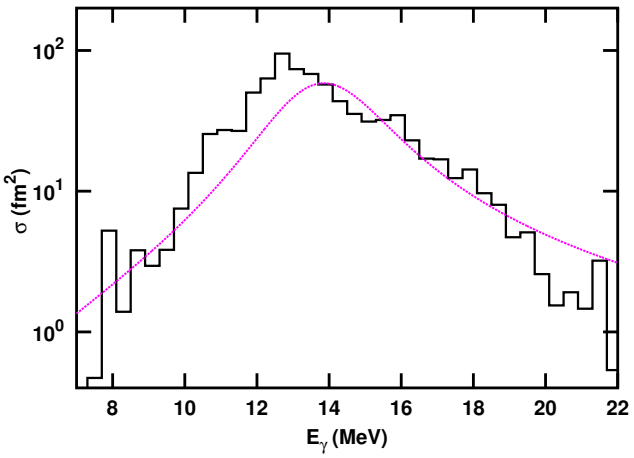

FIG. 4. (Color online) Dipole absorption from a shell model calculation for ^{208}Pb with configuration mixing [72](black histogram for E1). For comparison the Lorentzian from Fig. 3 is superimposed as dotted curve (magenta); it corresponds to Eq. (12) reduced to one pole

IV. GIANT DIPOLE RESONANCES IN HEAVY NUCLEI AND TRIAXIALITY

The coupling of dipole and quadrupole degrees of freedom in heavy nuclei has been discussed on the basis of hydro-dynamical considerations in the dynamic collective model (DCM) [60, 73]. Respective calculations were successfully compared to data for selected nuclei [74, 75]. The importance of the breaking of axial symmetry for the IVGDR shapes was mentioned for a few nuclei only [68, 76], but a full coverage of a wide range in the valley of stability is missing. The parameterization presented earlier [14] and again specified in this section is less ambiguous concerning the mode coupling, but it has the advantage of incorporating nuclear triaxiality explicitly by setting $k = 3$ in Eq. (11). For the resulting 'triple' Lorentzian (TLO) description the resonance energy E_0 is modulated by the ratios of the axis lengths R_i in the spirit of Eqs. (5 and 6). This direct incorporation of triaxiality makes TLO differ from previous attempts to obtain Lorentzian fits to photo-neutron data for a large number of heavy nuclei [12, 16, 55, 56, 77–79]. In many nuclei, especially those of intermediate Q_0, the local fits presented there may lead to a seemingly better agreement, but often they require quite unreasonably large values for the width of the IVGDR and for the integrated strength in comparison to sum rule predictions. Our earlier finding for two nuclides [14] is now extended in section VI to many more: If triaxiality is accounted for in addition to the quadrupole deformation a good description of IVGDR shapes can be obtained without treating the strength and width as free fit parameters. The deformation induced shift of the three axis lengths R_i versus the equivalent radius R_0 is obtained from Eq. (6), which uses results of a CHFB calculation [5, 69], as outlined in sections II and III. Hence, a global prescription to predict electric dipole strength may be derived from it, not limited to using local information for single nuclei. With this objective we point out that several components contribute to the apparent width of the IVGDR in heavy nuclei:

(a) Spreading into underlying complex configurations,

(b) Nuclear shape induced splitting,

(c) Fragmentation and

(d) Particle escape.

From calculations for heavy nuclei using the Rossendorf continuum shell model [80, 81] the escape width (d) in the IVGDR region was shown to be clearly smaller than the spreading width (a) derived by the global TLO-fit; a good agreement to data shows that Γ in Eq. (12) depends on the pole energies only and one global fit parameter. To fully understand a fragmentation (c) of the configurations belonging to *e.g.* the IVGDR a quantification of these configurations is needed, as is included in a microscopic calculation like the one presented in Fig. 4.

When a parameterization of the electric dipole strength in nuclei with non-zero Q_i is aimed for, the contribution of nuclear shape induced splitting (b) has to be treated sufficiently well. As proposed previously [14, 82, 83], a solution for this problem is found by allowing axial symmetry to be broken; this point will now be examined in further detail. As mentioned in section II accurate nuclear spectroscopic data suited to determine both deformation parameters are available only for a limited number of nuclei. The CHFB calculation [5] delivers prior information for Eq. (6) above, inserted to obtain the resonance energies in the sum of Lorentzian functions in Eq. (11). This procedure leads to a significant splitting into three equally strong IVGDR components which

increases with deformation. As will be summarized below in Fig. 25, for many nuclei the splitting between the three components is comparable in energy to their widths and thus not directly obvious from the data alone, especially in nuclides with $Q_0 \approx 200 - 300\text{fm}^2$. These are not rare as the clustering depicted in Fig. 1 shows, but the calculated triaxiality requires that all three axes are accounted for explicitly. This quite simple consideration explains the significant rise in apparent width as seen in Fig. 5 for the even Sm-isotopes with $N = 86$ to $N = 92$; ^{144}Sm was not included because of the uncertain cross section for the (γ,p)-reaction. The supplemental material

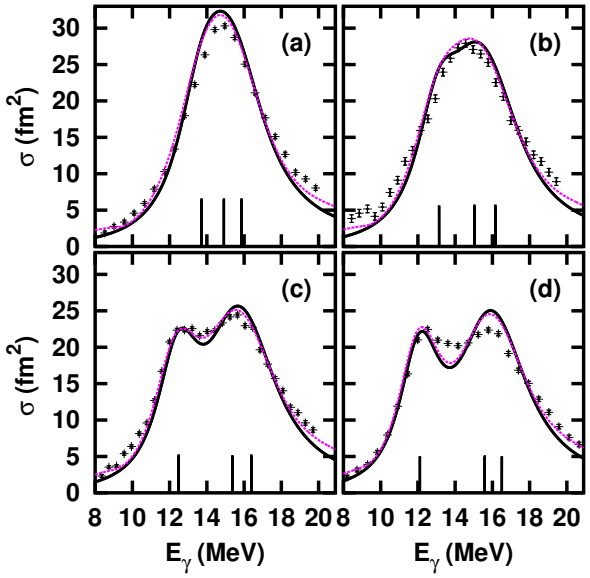

FIG. 5. (Color online) Photo-neutron production cross section ^{148}Sm [84] (a) to ^{154}Sm (d) in comparison to the TLO sum of three Lorentzians (drawn curve) with E_i indicated as black bars. The dashed (purple) curves indicate the effect of shape sampling [83, 85, 86]. As outlined in the next section the data were renormalized by a factor 0.9 and the calculations were folded with a Gaussian to simulate an experimental beam spread of $\sigma \cong 0.3$ MeV [87]. Panels (b) and (c) depict the situation for ^{150}Sm and for ^{152}Sm, respectively.

based on the CHFB-calculations [5] does not only list the mean values for the deformation parameters as obtained via the GCM, it also gives their variances as resulting from quantum mechanical zero point oscillation. The respective Gaussian distributions obtained thus allow an instantaneous shape sampling (ISS) as shown earlier [85] for isotope chains Mo [83] and Nd [86]. There the impact of ISS on the height of the low energy tail and thus on radiative capture was demonstrated to be negligible. Results for the Sm chain as shown in Fig. 5 indicate a minor influence as well: the drawn black curves correspond to the TLO-prediction and the dashed purple curves stem from calculations including ISS.

Special care is needed for nuclei near closed shells: The CHFB calculations do not fully account for the very deep mean field potential in such nuclei and thus they produce too much of collectivity [69]. Following what is said there, a reduction for nuclei only δ nucleons away from a shell a factor for the β-deformation [5] of $0.4 + \delta/20$ is applied for $\delta \leq 10$. This expression is used for protons as well as neutrons and the larger of the two correction factors is taken; it results in a reduction of the predicted [5] β-values by 40, 30, 20 and 10% for the isotopes ^{148}Sm, ^{150}Sm, ^{152}Sm and ^{154}Sm and the corresponding agreement to the IVGDR data is shown in Fig. 5. The extension of CHFB to non-spherical nuclei introduces no extra free parameters in addition to the global ones of the Gogny-force [5]: A fit to the IVGDR energies and widths succeeds with only the four parameters introduced in Eq.(12), two of which are known from LDM mass fits. As will be demonstrated in section VI the strict distinction between damping or spreading and the deformation induced splitting allows to neglect a photon energy dependence of the width for all nuclei treated there. Thus the only local parameters for individual nuclei are the axis ratios calculated by CHFB [5] and the widths Γ_i in Eq. (12) vary only with the pole energies E_i (and not with A and Z). This opens the possibility for a global prediction of photon strength also for heavy exotic nuclei and has the potential of consistent predictions for radiative capture processes, where full satisfaction was not reached with presently available methods [88]. For an extension to energies below the neutron emission threshold S_n modes in addition to the IVGDR have to be investigated concerning their contribution to photon absorption.

V. STRENGTH FUNCTIONS FOR ISOVECTOR ELECTRIC DIPOLE AND ADDITIONAL MODES

The height of the low energy tail is nearly proportional to the IVGDR width and it depends weakly on its deformation induced splitting. A consequence hereof is a nearly full independence of the strength on any free parameter. In photon scattering experiments in this energy range mainly narrow peaks were observed above background and these were interpreted as strength of apparently other character than isovector electric dipole [16–20]. In the literature the excitation energies of such modes are discussed in much more detail as compared to the strength observed. Even if it has minor importance for total photon absorption and the sum rules, it may influence the decay of the compound nucleus and consequently also the cross sections of capture reactions. Here at least their average electromagnetic strength has to be regarded. For an assessment of the agreement between TLO and experimental data the strength eventually adding to the IVGDR tail has to be characterized; if it is not of electric isovector kind it has to be described separately from IVGDR, which we propose to be in accord to TLO. As a first step of such a characterization we have derived phenomenological expressions for these 'mi-

nor' modes in their A-dependence and compare them to data, which are partly obtained at the ELBE facility at Dresden and partly derived from published work, as specified below. Following a presentation of various modes we list the obtained parameters in Table I and consider this as a basis for eventual theoretical work adressing especially strength issues.

A direct relation exists between ground state transition widths, summed for all levels within an energy interval Δ_E, and the strength functions $f_{E\lambda}$ (in MeV$^{-(2\lambda+1)}$) defined as follows:

$$f_\lambda(E_\gamma) = \frac{\sigma^\lambda_{abs}(E_\gamma)}{(\pi\hbar c)^2 g_{eff} E_r^{2\lambda-1}} = \frac{1}{\Delta_E}\sum_r \frac{\Gamma_{r\gamma}}{E_\gamma^{2\lambda+1}} f_\lambda(E_\gamma) \cong \frac{\langle\Gamma_{r\gamma}(E_\gamma)\rangle}{D_r \bar{E}_\gamma^{2\lambda+1}} \quad (13)$$

The first part of Eq. (13) relates the strength function to the photon absorption cross section $\sigma^\lambda_{abs}(E_\gamma)$ which is limited by sum rules. Strength functions $f_\lambda(E_\gamma)$, were introduced [16] as statitical average for all electromagnetic processes proceeding by multipolarity λ. To use the strength functions $f_\lambda(E_\gamma)$ for excitation as well as decay processes and thus connect photon scattering to radiative capture and photonuclear processes one has to suppose them to be independent of the direction of the process (Axel-Brink hypothesis)[16, 89, 90]. The second line of Eq. (13) directly relates f_λ to the electromagnetic decay widths of the resonant levels r in the integration interval Δ_E. Strength information can hence be obtained by summing spectroscopic width data (in MeV) over a given energy range (also in MeV) running from $E_\gamma - \Delta E/2$ to $E_\gamma + \Delta E/2$. Their average distance is D_r and for the sum in Eq. (13) all levels within this interval are included; the quantum-mechanical weight factor g_{eff} will be discussed with Eq. (15).

Electric dipole strength below the IVGDR

A low energy dipole mode was predicted to be formed by E3 strength coupled to low energy quadrupole modes [11]. In many even-even nuclei rather strong photon absorption into 1^--levels with 1MeV $< E_x <$ 4MeV has been observed [91]. As a correlation of E_x to the sum of the excitation energies of the low collective 2^+ and 3^--modes and similar strength for odd and even nuclei was observed, this phonon coupling mode is considered well established [91]. These photon scattering studies revealed fragmentation away from closed shells and especially in odd nuclei; it may cause a non-observation of small-strength components. To estimate the centroid energy E_{qo} the sum energy of the 1st 2^+-level [24] and the corresponding value for the octupole (3^-) excitation [92]; for exotic nuclei theoretical approximations are available [5, 93].

Already long ago "intermediate structure" observed by photon scattering in the energy range 5 to 8 MeV was discussed in detail [80] and the concept of photon strength functions $f_\lambda(E_\gamma)$ was introduced to quantify its strength. For photon scattering by Zr and Sn [15] as well as for $A \approx 200$ [94] this issue was addressed with special care in the photon detection. As mentioned there, the contribution of the quasi-continuum below the lines is significant even after the real background due to unwanted radiative processes in the detector and the near-by environment was identified and subtracted. More recently [95, 96] the non-nuclear scattering by the target and the near-by environment was numerically simulated, but eventually minor strength - often denoted as PDR ('Pygmy Dipole Resonance') [20, 97] - was quantified mainly by integration of the yield observed by Ge-detectors in narrow peaks. The electric dipole strength outside of the IVGDR may have isovector or isoscalar character and a distinction by experiments with isoscalar beams was proposed [20, 98, 99]. Hints for the isoscalar character of electric dipole strength may indicate non-uniform proton-neutron distributions or compressional modes. Strength between $E_x \cong 5.5$ MeV and the neutron separation energy S_n was shown to be of isoscalar nature in ^{40}Ca, ^{58}Ni, ^{90}Zr and ^{208}Pb by the coincident observation of inelastically scattered α-particles and de-excitation γ-rays [98].

In the present study the various results reviewed recently [20] for this energy range are tentatively separated into two components and named low and high energy pygmy mode (PM). The parameters given in Table I for the strength integrals should be understood as approximate. As becomes obvious in subsequent figures, the low energy PM (a seemingly resonant strength near $0.4 \times E_{IVGDR}$) appears to be of similar magnitude for many different A, when compared to the IVGDR. Experimental "evidence for a 5.5-MeV radiation bump" in nuclei near Pb, an intermediate structure named 'pigmy' [16] 40 years ago, was recently extended [96] to isotopes in the N = 50 and N = 82 region, and this suggests our nomenclature as high energy PM.

Magnetic Dipole Strength

Magnetic (M1) strength is weaker as compared to E1 [79] and , as outlined in a recent review [18], its spin flip component occurs at higher energy than collective orbital magnetic strength (scissors mode). The latter is strong in nuclei with a large quadrupole moment and high resolution photon scattering data [95, 99–101] show the strength of M1 transitions to be below that for E1 for energies above 2 MeV. The magnetic strength in Table I is mainly derived from a review published recently [18]. A surprisingly high magnetic strength was used in calculations for Zr-isotopes [102], although it superseded this systematics by a factor of ≈ 3. Combined to a rather low E1-strength as derived from a HFB+QRPA calculations [103] a suitable agreement to capture data results;

in view of the very large M1-component used the underlying E1 model may have to be questioned. A statistically significant information on E1 and M1 transitions was collected from a nuclear data base [104] to construct Fig. 6; an ensemble of nearly 3000 transitions in heavy nuclei with $80 < A < 180$ was used. The M1-strengths

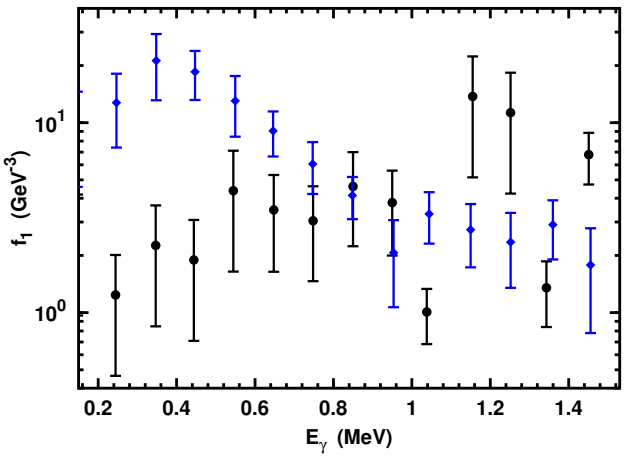

FIG. 6. (Color online) Strength functions for from a data compilation [104, 105]. The points depict the averages for M1 (blue diamonds) and E1 (black circles) and the vertical bars indicate 20% of the root-mean-square deviation of the data in each bin from the averages.

$f_{M1}(E_\gamma)$ are apparently considerably larger than the E1-strengths $f_{E1}(E_\gamma)$ for E_γ below 1 MeV whereas above the E1 strength becomes stronger and seems to approach the tail of the IVGDR. A direct measurement of the transition strength contributing to the decay width in the high level density region near S_n was possible by using experimental information gained in ^{143}Nd(n,$\gamma\alpha$) experiments [106, 107]. In view of Fig. 6 this "low energy" strength is likely to be mainly M1 as pointed out before [108], but E1 was occasionally assumed to be the main component [52, 79]. Recently very low energy M1 transitions resulting from orbital rearrangement have been predicted by shell model calculations for Mo-isotopes [109] to compete to E1 below 3 MeV.

Electric quadrupole modes

Low energy E2-transitions can be considerably enhanced and have played an important role in the spectroscopy of heavy nuclei – as discussed in section II. The photon absorption cross sections can be derived from Eq. (9); they have been found to be small as compared to E1 absorption [110] in the energy region near S_n. This is also true for the absorption into the third 2^+-state predicted for triaxial nuclei [5, 33] to have a B(E2) value up to 7% as compared to the first. Extending previous work [14, 55, 110, 111] the influence of quadrupole giant resonance (QDR) contributions to photon absorption was investigated by us; information for quadrupole strength comes from sum rules and theoretical predictions [10, 110, 112] adjusted to electron scattering data [53, 54, 113]. Strength modifications at higher energy due to the isovector IVGQR appear to be important, as seen in the upcoming figs. 7 to 24. Here f_{E2} was multiplied with E_γ^2, the additional energy dependent phase space factor for absorption and decay, to allow a visual comparison to f_1; for the calculation of the integral $I_{E2} = I_c$ (as listed in Table I) the correct decay width is used in Eq. (8). The isoscalar ISGQR lies not far from the pole of the IVGDR such that it adds to the strength observed there, causing a small deviation from TLO.

The approximations used in Table I for the integrals of the E1, E2 and M1 components were derived through a comparison to respective observations [18, 79, 101] under respect of the above mentioned information. The resulting parameters for these "minor" contributions to the photon strength function are listed there; independent of an interpretation of these modes a Gaussian seems justified to describe them. No arguments were found, why Lorentzians should be preferred; this differs from the IVGDR, where a Lorentzian with energy independent width is appropriate [61, 67]. Separate Gaussian distributions

$$f_\lambda(E_\gamma) = \frac{1}{(\pi\hbar c)^2 g_{eff} E_\gamma^{2\lambda-1}} \frac{I_c}{\sqrt{2\pi\sigma_c^2}} \exp\left(\frac{-(E_\gamma - E_c)^2}{2\sigma_c^2}\right) \quad (14)$$

for each of them are used and this supresses unobservable strength in long tails; the parameters were selected to somewhat overpredict available data after the TLO-integral over the energy interval is subtracted [96]. Table I lists the cross section peak integrals I_c as well as the centroid energies E_c and the standard deviations σ_c (in MeV) as discussed above. The I_c in Eq. (14) as well as in Table I are sums over many individual levels within the Gaussian like in Eq. (11) for the IVGDR and at variance to Eq. (7), valid for a single level. In the next sections the results corresponding to a sum of TLO and the 6 Gaussians for the "minor" modes are shown as blue lines in figs. 7 to 24. The average quantity f_λ is depicted, which usually [16] is assumed to be insensitive to details of the nuclear excitations and hence one approximates collective electromagnetic transition strengths of energy $E_\gamma = E_r$ - E_f to be independent of the energies E_r and E_f by using $f_\lambda(E_\gamma)$; together with the notion of f_λ being valid for excitation and decay (Axel-Brink hypothesis) . It should be stressed, that the contribution of all "minor" modes to the sum rule integral in Eq. (10) is weaker by at least one order of magnitude as compared to the IVGDR sum. The relative importance of the components for cross sections eventually calculated with expressions presented here may be found in a letter published recently [114], where approximate expressions for the level density and the cross section of radiative capture were combined to TLO and the minor modes to derive a global comparison to experimental data.

Component parameter(units)	multi-polarity	E_c (MeV)	I_c (fm^{2}MeV)	σ_c (MeV)
low E_x pygmy mode	E1	$0.43E_0$	$7\ \frac{Z(N-Z)}{A}$	0.6
high E_x pygmy mode	E1	$0.55E_0$	$13\ \frac{Z(N-Z)}{A}$	0.5
$0^+ \leftrightarrow (2^+ \times 3^-)_{1-}$	E1	$\frac{140}{N}(1+\frac{107}{Z})$	$0.006ZA\beta$	0.6
orbital (scissors) mode	M1	$0.21E_0$	$0.033ZA\beta$	0.4
isoscalar spin-flip	M1	$42A^{-1/3}$	17	0.8
isovector spin-flip	M1	$47A^{-1/3}$	27	1.3
low E_x quadrupole	E2	$19A^{-1/3}$	$0.1\ \frac{\alpha(\pi R_p E_\gamma)^2 Z^2}{(3Am_pc^2)}$	1.0
ISGQR	E2	$63A^{-1/3}$	$2\ \frac{\alpha(\pi R_p E_\gamma)^2 Z^2}{(3Am_pc^2)}$	1.0
IVGQR	E2	$48A^{-1/6}$	$\frac{\alpha(\pi R_p E_\gamma)^2 Z^2}{(3Am_pc^2)}$	1.8

TABLE I. Parameters of an upper limit for three minor electric and three magnetic dipole modes to the dipole strength function to be calculated with a Gaussian (Eq.14). A very similar shape near the peak is reached for a Gaussian with a standard deviation σ_c, which is larger by a factor 2.5 as compared to the width Γ of a Lorentzian. Three GQR modes are also listed, which are seen in photon absorption as well; they are proportional to the square of the nucleus' charge radius R_p (rms).

VI. ELECTROMAGNETIC STRENGTH IN THE IVGDR AND BELOW

The TLO ansatz and the presented phenomenological description of 'minor' strength do not aim for a full theoretical understanding of the coupling between the IVGDR to quadrupole modes or other excitations, but only for a prediction of photon strengths, which is global and hence extendable to many nuclides. In view of the already previously observed [16] "difficulty of accounting for the bump with the aid of a smoothly varying strength function", we clearly distinguish between the Lorentzian tail and "minor" intermediate strength. Such an ansatz was successfully applied to near (semi-)magic nuclei [15, 94], but later opposed heavily [59, 79, 115] on the basis of the KMF model [52] and data for nuclei with larger Q_0. It will be shown that giving up axiality, *i.e.* using TLO, describes existing data at least as well these 'newer' parameterizations.

Several facts had to be regarded in the use of published photo-neutron or photon absorption experiments:

1. Considerable discrepancies were reported for experiments performed *e.g.* at different laboratories [102, 116, 117]; in some cases energy calibrations may differ somewhat.

2. Photo-neutron data were often obtained by using quasi-monochromatic photon beams with a rather wide energy distribution, which is incorporated by folding the calculations with a Gaussian of width σ= 0.3 MeV, a value not as large as some recently made guesses [118, 119]. Also in the case of a bremsstrahlung distribution used as photon source quite some uncertainty may arise [120].

3. It has been found by various studies [116, 119, 121–125], that photoneutron cross sections determined at Saclay around 1970 should be reduced. The necessary reduction is probably related to difficulties in the analysis of multi-hit events in the neutron detector array [119, 123]. In accordance to a precision study [116], confirmed by results [83, 126] from the radiation source ELBE, the photo-neutron data of that origin are hence multiplied in this work by 0.9, considered as suitable for various A.

4. In a number of cases the (γ,p)-channel exhausts a significant portion of the photo-absorption cross section [56, 78, 83]. It was shown in an earlier paper [83], how the eventual influence of all open channels on the extraction of the absorption cross section from the existing data is tested by Hauser-Feshbach calculations.

5. At higher energy the competition by the (γ,2n) channel becomes important and that requires involved subtraction procedures [75], which may be questioned [118, 119].

6. Most of the targets used contain isotopic contaminations, and when some of them have a lower S_n (like many odd isotones) the low energy yield has to be corrected [83].

7. Below and above the pole of the IVGDR contributions from the giant quadrupole (GQR) modes may cause effects, and sufficiently accurate GQR-data could be very helpful for future work.

8. In heavy nuclei various excited states may exist aside from giant resonances, which cause observable photon strength also below the neutron threshold. It adds to the IVGDR tail not always smoothly, as Porter-Thomas fluctuations [90] may randomly create strong peaks in spectra from a quasi-continuum of weakly populated levels.

In the IVGDR region averaged experimental photoneutron data obtained with quasi-monochromatic photons from positron annihilation in flight are available [77, 78, 104]. Such data do not exist for all stable isotopes and for some nuclei the total photon cross section

has been studied by an absorption technique. These data may serve for a consistency check in spite of systematic errors due to the need to subtract the strong atomic absorption. Items 2 to 5 of the list above influence the representation of the IVGDR peak region, but their effect on the tail a few widths Γ below the pole is less important then items 6 and 8.

Photon strength data for energies below S_n are even rarer [14]. Similar as in many photo-neutron studies experiments with quasi-monochromatic beams are performed to gain information on absorption from photon scattering: In early experiments the tagging system at Urbana was used [15, 94] and an increasing number of measurements were done at the laser-photon backscattering facilities HIγS (High Intensity γ-Ray Source) at Duke University [110, 127] and AIST (National Institute of Advanced Industrial Science and Technology) in Japan [117]. The photon intensities from these are not well known and bremsstrahlung data eventually serve for normalization. Results from scattering have to be corrected for branching to other than the ground state and in various cases the bremsstrahlung continua also feed higher excited levels and their decay yield has to be subtracted. For a globally applicable quantification the yield not seen as individual spectral lines in a Ge-detector (looking like quasi-background) has to be taken into account [95, 96]. In the case of less complex spectra use can be made of data from the decay to well isolated levels [128, 129]. More sophisticated schemes as developed *e.g.* at ELBE [83, 130, 131] are based on statistical considerations already formulated some time ago [15, 16]. Due to the fact, that the electromagnetic strength is responsible for the absorption as well as the emission of photons, an iterative procedure can lead to a self-consistent solution [96, 131, 132]. Here, nuclear level densities enter which often were taken from predictions and extrapolations eventually questioned. In view of a new formulation [114] including an collective enhancement of level densities a reduction of 30% in the f_λ as compared to published values was applied in the case of some ELBE-data as mentioned in the respective figure captions. In principle, also photon yields observed after nuclear reactions can deliver strength-information, when it can be normalized via an "external" fixed point. In the case of resonant neutron capture this is realized by "using the absolute gamma-ray intensities due to captured thermal and resonance neutrons" [115]. But the observed spectra [58] indicate, that the strength published was observed only because it was significantly stronger than the one buried in the experimental background (*e.g.* due to Compton scattering in the photon detector).

The subsequent compilation presents in figs. 7 to 24 photon strength function data and a comparison to the TLO parameterization with three IVGDR pole energies induced by the non-axiality. Here deformation parameters are taken from the available CHFB-calculations [5] together with globally determined values for c_w in Eq. (12) and an effective mass quantifying [14] the centroid E_0. The (black) dashed lines represent the prediction of f_{E1} thus derived with the resonance integral from Eq. (11) (in accordance to the TRK sum rule) equally divided among the three poles of TLO. In all these figures the three are indicated as black bars at the energy axis. It is worth mentioning that the absolute heights in the low energy slope are nearly unchanged by the splits, albeit the apparent peak-height depends on it. As shown previously [131], the effect of the photon strength on radiative neutron capture is strongest in the tail region below the neutron binding energy S_n. Here up to eight additional "minor" strength components may be of importance; they have been detailed in section V. For a specification of their energy, strength and width we have used published data as listed with the figures. But the available information is by far not detailed enough to derive a systematic parameterization to evaluate their eventual influence on neutron capture with high precision. This is demonstrated by the experimental data inserted in the figures; the result of our adjustment of the relevant parameters to derive an approximate agreement is depicted by a full (blue) line. Like for TLO only globally fitted quantities enter the calculations for these plots; they are compiled in Table I. The plots start at 3 MeV as below Thomson scattering by the nuclear charge surmounts the IVGDR tail and especially the zero at $E_\gamma = 0$ in Eq. (11).

For the nuclei to be discussed photo-neutron data and results for energies below S_n are available in a wide range of A, Z and Q_0. A comprehensive collection of photon absorption data are available from the EXFOR data base [104], for which they were extracted from original work. To improve the visibility of the data points, some of the excitation functions have been re-binned to around 0.6 MeV/bin, and points of no significance were suppressed, *e.g.* when their uncertainty is comparable to the value. The subsequent figures will demonstrate what features of photon strength can be derived experimentally, and how well systematic trends become visible. For nuclides with $A <\approx 60$ channels competing to (γ,n) may cause difficulties for the extraction of the total photo-nuclear cross section [78] and hence the photon strength. In view of an increase of this problem with falling A the reason for not extending the study to A as low as 60 seems reasonable.

Even-even nuclei

In ^{78}Se a significant increase over the extrapolated tail is observed from photon scattering investigated at the radiation source ELBE for $7 < E_\gamma < 10$ MeV, although these data [131] were reduced by a factor of 0.7. This is a correction for the disagreement of the level density ansatz used in the data analysis [131] with the one published recently [114]. In any case, there is an overshoot above TLO, which is not completely acconted for by our phenological ansatz for 'minor' strength.

For ^{88}Sr [14, 114], as well as for $^{92-100}$Mo [83, 130] mi-

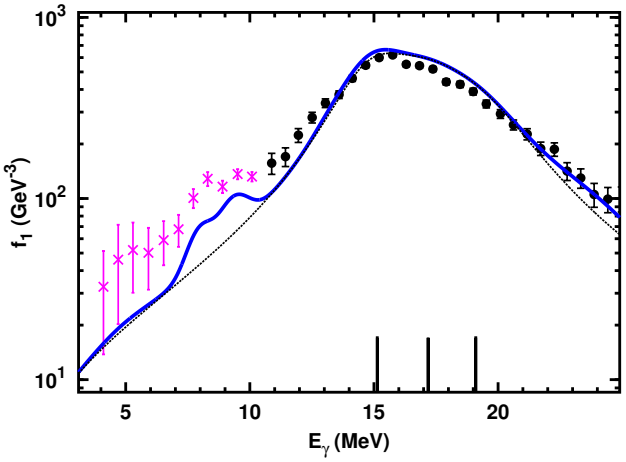

FIG. 7. (Color online) Photon strength function for ^{78}Se: the TLO-prediction is depicted as dashed black line and a full line in blue represents the approximate influence of minor strength. Photoneutron results (black dots [133]) are shown in comparison as well as photon scattering data at lowE_γ; these (x-symbols in magenta) were obtained with bremsstrahlung from ELBE [96, 131] and reduced by 30% in view of a new level density ansatz [114].

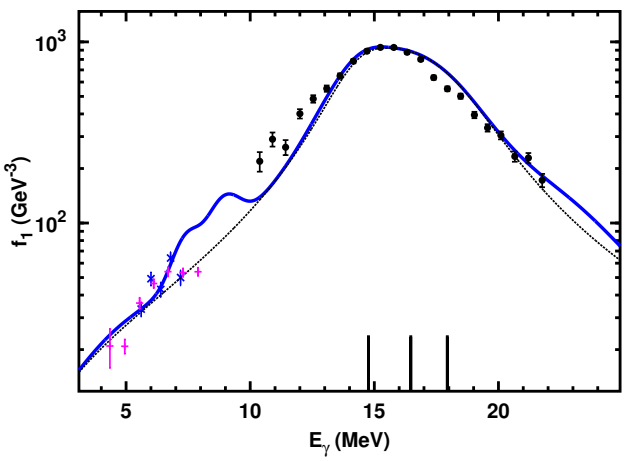

FIG. 8. (Color online) Photon strength for ^{98}Mo from photoneutron data [137] (black circles) in comparison to the sum of three Lorentzians (TLO) as described for Fig. 7. The data below 9 MeV are from elastic photon scattering ^{98}Mo(γ,γ) observed with monochromatic photons [134] (blue x) or bremsstrahlung [130] (magenta + symbols, modified by 0.7).

nor strength was observed at low energy similar to ^{78}Se. Work on photon strength performed at the ELBE facility was already published previously; there our experiments and their analysis are described in detail. A width independent of E_γ was used, a need to not assume axiality is observed and the integrated cross sections obey the TRK sum rule. The similarity between the low energy slopes in the experimental data of all Mo isotopes led to the suggestion [14, 83] of an extrapolation with energy independent width under the assumption of broken axial symmetry. Looking at ^{98}Mo in the tail below 10 MeV shows that bremsstrahlung data corrected statistically for inelastic scattering [83, 130] are very close to newer results obtained with quasi-monochromatic photons [134]. At variance to this agreement photon strength function derived from gamma decay after inelastic ^{3}He scattering [135] are nearly a factor of 3 smaller at 7 MeV as compared to the data as shown in Fig. 8 and this may indicate, that the so-called Oslo method may suffer from the uncertainty in level density mentioned above. The recently revised data [136] agree around 7 MeV with our photon scattering results and thus also with the TLO prediction with minor strength added. These new data overshoot at higher E_γ and are lower by $\approx$ 40% near 3 MeV. In the nuclides $^{94-96}$Mo this was shown to be in accord to a shell model calculation for M1-strength [109].

Quasi-elastic photon scattering from natural Sn has been studied long ago [15] at the tagging set up installed at Urbana and "intermediate structure" in addition to the IVGDR tail has been identified. The absorption cross sections were derived from scattering data [15]; their branching correction by inserting constant average resonance widths may overestimate σ_{abs} by at most 20% [15]. To improve the overlap with the $(\gamma$,n)-data a reduction by 0.8 was applied in Fig. 9 and the resulting values are shown together with the cross section for ^{118}Sn $(\gamma$,xn) [138], obtained with positron annihilation in flight; the surprisingly large strength near 10 MeV may be related to a target admixture of odd isotopes, similar to what was worked out for Mo targets [83]. Recent experiments with laser backscattered photons [117], which cover the threshold region, support such an assumption for ^{118}Sn. From a high resolution photon scattering experiment [129] with correction for branching losses a strength enhancement near 6.5 and 8 MeV was reported for ^{116}Sn and ^{124}Sn, similar to what is shown here for ^{118}Sn. A recent study of ^{112}Sn and ^{120}Sn [139] uses statistical corrections for inelastic scattering as proposed earlier [15, 130] and again finds similar dipole strength as reported earlier. In addition, the last-mentioned investigation has detected by a fluctuation analysis the need to increase the final photon strength by nearly a factor of two with respect to the sum of peaks observed in the spectra and resolved with $\approx$ 2 keV (FWHM) energy resolution. Whereas data on f_γ derived at Oslo for various Sn isotopes and other nuclides with ^{3}He-induced reactions show significant differences from the photon scattering data shown here, the recent reanalysis for ^{118}Sn [140] does no longer - as depicted in Fig. 9. The overshoot seen at the higher energies can be explained by the influence of the giant quadrupole resonance and is of no importance for the discussion here.

In Fig. 10 results from photo-neutron emission from ^{nat}Te, multiplied by 0.9 – as done in general for data from Saclay – agree well to TLO above the IVGDR peak. The various isotopes in the target may cause a widening

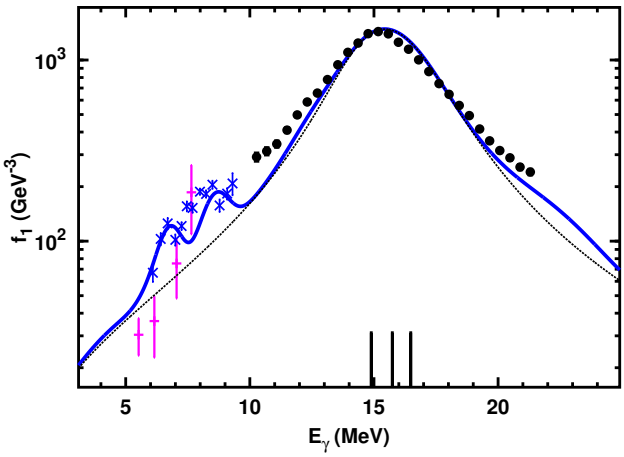

FIG. 9. (Color online) Photon strength for ^{118}Sn from photon scattering [15] (blue x symbols) at low and photo-dissociation [138] (black circles) at higher energy in the IVGDR range. The data are compared to TLO (see the caption of Fig. 7). Recently reanalyzed data [3] from gamma decay after ^{3}He induced reactions are shown as well (+ symbols in magenta with large uncertainty bars).

of it and on the low energy side of the peak the isoscalar component of the GQR is expected from the systematics for this mode; its influence on the photoneutron cross section is not completely clear. The low energy data support the finding of "intermediate structure" or "pygmy" strength as observed since long [15, 16, 94] near $0.4E_0$, also seen in Figs. 9 and 11 and to some extent in the data below 10 MeV for all nuclei presented here.

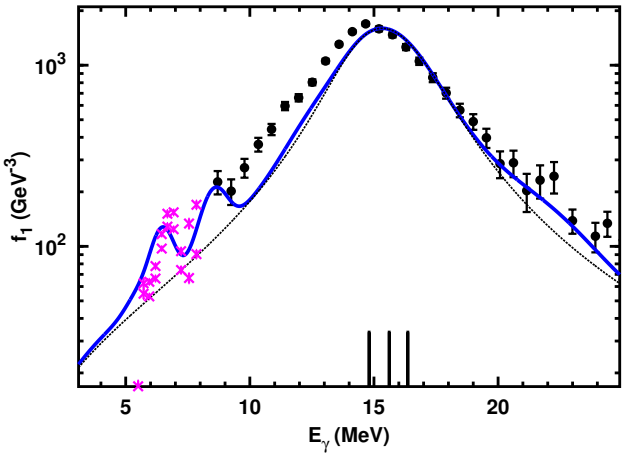

FIG. 10. (Color online) Photon strength for ^{130}Te calculated as sum of three IVGDR-Lorentzians (TLO)(see the caption of Fig. 7) in comparison to data from photoneutron production in natural Te [138] (black circles). The data below S_n (x, magenta) are from a careful analysis [141] of scattering data taken with quasi-monoenergetic photons, yielding lower and upper limits for the photo-absorption cross section.

For ^{138}Ba scattering data have been taken with quasi mono-energetic photons at the laser backscattering beam at HIγS [127], whereas a bremsstrahlung experiment at ELBE was performed with ^{136}Ba [132]. As one can assume that the two data sets result in very similar absorption cross sections, they are shown together in Fig. 11.

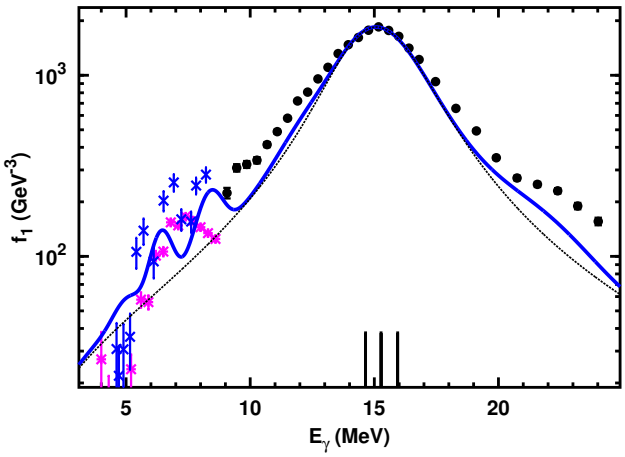

FIG. 11. (Color online) Photon strength derived by photoneutron production on ^{nat}Ba [122](black circles) in comparison to TLO for the IVGDR for ^{138}Ba (see the caption of Fig. 7). Photon scattering data for $E_\gamma < S_n$ are shown as blue x-symbols [127] and magenta asteriks for ^{136}Ba [132] reduced by a factor 0.7.

For the nuclides to be discussed in the following (^{146}Nd to ^{190}Os) photon strength information for $E_\gamma < S_n$ was obtained from individually known branching ratios of gamma transitions following neutron capture via resonances near S_n [16] or by analyzing gamma spectra following average resonance capture (ARC) [115] to reach the nucleus in question. Experimentally an inspection of the gamma-ray angular distributions assures $\lambda = 1$, and the decay multipolarity (E1 or M1) is derived by using several neutron energies [59, 79]. Inserting these widths and the average level spacings into Eq. (13, second line) results in $f_\lambda(E_\gamma)$, but this relies on a known level density $1/D_r$ [58, 59, 79, 114, 142, 143].

In Fig. 12 the case of ^{146}Nd is shown and the triaxiality in TLO leads to a reasonable description of data in the region of the IVGDR as well as below. In accord to Eq. (11) and (12) comparatively small Γ_i of 2.82, 3.33 and 3.76 MeV are used without a decrease with E_γ. In previous work [55, 56, 77] a single Lorentzian (SLO, $k = 1$) was proposed for ^{146}Nd together with $\Gamma_{IVGDR} = 5.74$ MeV, also shown in Fig. 12 as magenta curve. It indicates that such a fit leads to a large resonance width Γ, as it emphasizes the pole region. Only with a decrease of the IVGDR width with photon energy, as was assumed [55, 58, 79, 144] in KMF-type analyses [55], agreement to the low energy data near 5 MeV is reached in spite of the large value for Γ. For even lower energy it was proposed

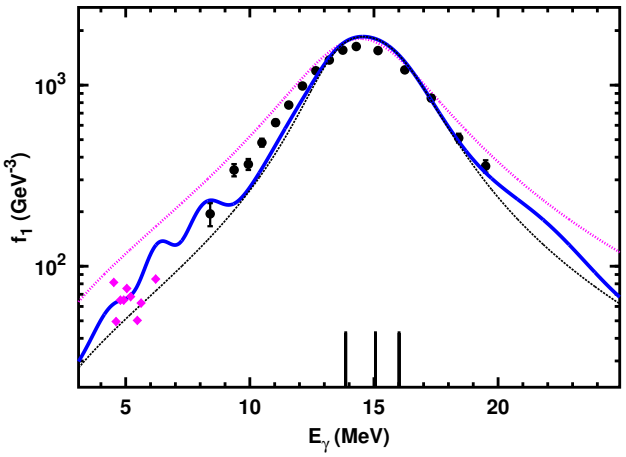

FIG. 12. (Color online) The photon strength for ^{146}Nd in comparison to TLO for the IVGDR (dashed line in black). The data above S_n are from photo-neutron production [121] and the ones below (magenta diamonds) are derived from gamma decay subsequent to ARC by ^{145}Nd [115]. The dotted line in magenta results from a fit to these data with one pole only [56] and the comparison to TLO is depicted as blue line (see caption of Fig. 7)

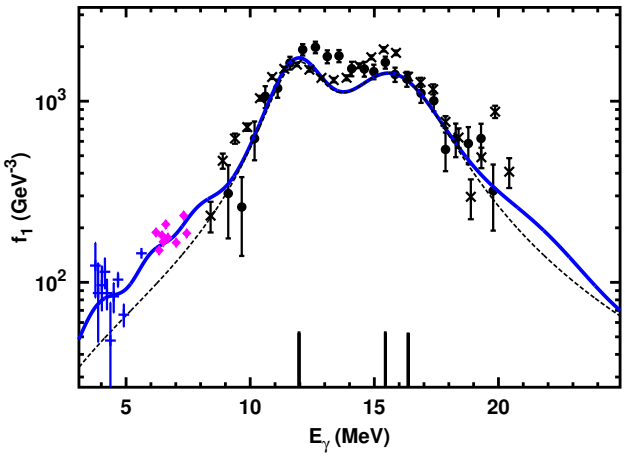

FIG. 13. (Color online) Photon strength for ^{156}Gd in comparison to TLO (see the caption of Fig. 7). Data for 6-8 MeV ([115] magenta diamonds) are derived from ARC as well as those below, which are for ^{157}Gd ([59] blue +). The photon absorption ([145] black circles) and photo-nuclear data ([146] black x-symbols) do not fully agree in the peak region.

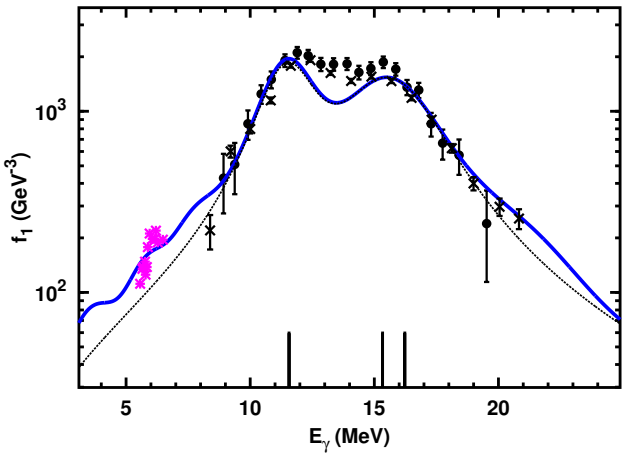

FIG. 14. (Color online) Photon strength for ^{168}Er derived from ARC data (magenta * symbols [115]) and from the cross section of photon absorption (black dots [145]) in comparison to TLO (dashed curve in black). Shown as full line in blue is the prediction with minor strength and photo-neutron data for $^{\rm nat}$Er(γ,xn) [147] are depicted as black x-symbols.

to add a component to the Lorentzian which violates the Axel-Brink hypothesis; this has allowed to assign E1-character to the data from ^{143}Nd(n, $\gamma\alpha$) [106, 107] with their strength observed even below 1 MeV. But this neglects the fact, that M1 radiation should be favored [108], similar to what was indicated theoretically for $^{94-96}$Mo [109].

Figs. 13 and 14 show results of two different experiments for the IVGDR range; they were selected as an example for experimental uncertainties to be aware of in discussions about details of the dipole strength: The data with the larger error bars were obtained by photon absorption with subsequent subtraction of the strongly dominating absorption by the atomic shell, which has to be determined by a precise calculation. The other data are from photo-neutron experiments; the deviation in the minimum near 14 MeV may result from a large energy width of the photon beam, but still the agreement to TLO is remarkable. Also for low energy data obtained with different methods are depicted in Figs. 11 and 13. In view of the large Porter-Thomas fluctuations, which have been only partly averaged out by re-binning the plots, they agree to each other; they also have reasonable accord to our prediction after 'minor' strength was added to TLO following the global parameters of Table I. If photon scattering experiments covered the respective energies intermediate "pygmy" structures at $E_\gamma \approx 0.4$ and/or $0.6E_{IVGDR}$ are seen (figs. 9 to 11, 13, 16 and 17). Enhanced gamma-strength was seen only at $E_x \approx 0.4E_{IVGDR}$ from α-scattering experiments with subsequent direct decay to the ground state [98, 99]. As listed in Table I the measurement using isoscalar projectiles indicates an isoscalar character [20] for this low energy pygmy mode - in accordance to recent calculations ([150]). Already many years ago, experiments with tagged photons [94] have identified a resonance-like structure in the cross section of photon scattering on targets in the vicinity of ^{208}Pb, and the case of Hg is especially significant: TLO with its small Γ predicts a considerably smaller cross section as compared to the low energy pygmy resonance near 5.7 MeV, which clearly surmounts the smooth tail. Here it was shown [94] to be impor-

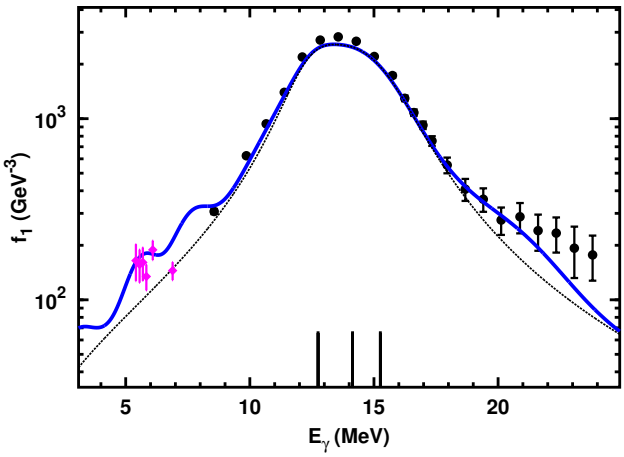

FIG. 15. (Color online) Photon strength for ^{190}Os derived from ARC data (magenta diamonds [148]) and from the cross section of photo-neutron production (black dots [149]). For comparison the TLO result is shown as before (see the caption of Fig. 7).

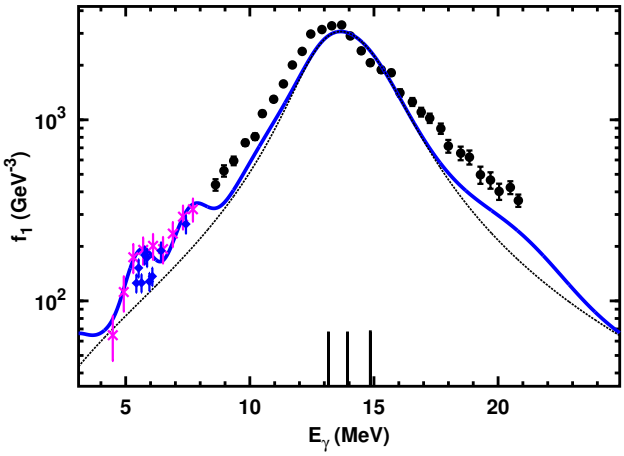

FIG. 16. (Color online) Photon strength for ^{196}Pt derived from ARC data ([115] blue diamonds) and from the photoneutron cross section ([151] black dots) in comparison to TLO (see the caption of Fig. 7). Photon scattering data ([132] magenta x-symbols) are reduced by 30% in view of the "new" ansatz for the level density [114].

tant that photon scattering yields are properly corrected for inelastic scattering. In ^{208}Pb the energy of such minor modes lies in a region of small level density and hence very large spacing between 1^--levels and it is intriguing to compare the strength function in the strong 1^--levels at 5.29 and 5.51 MeV [72, 153] to the pygmy resonance in Hg: They are very similar in energy and energy-integrated strength, and can eventually be identified as one type of pygmy resonances [154]. In this mass region Porter-Thomas fluctuations have a large effect [152, 155–157] because of low level density reaching

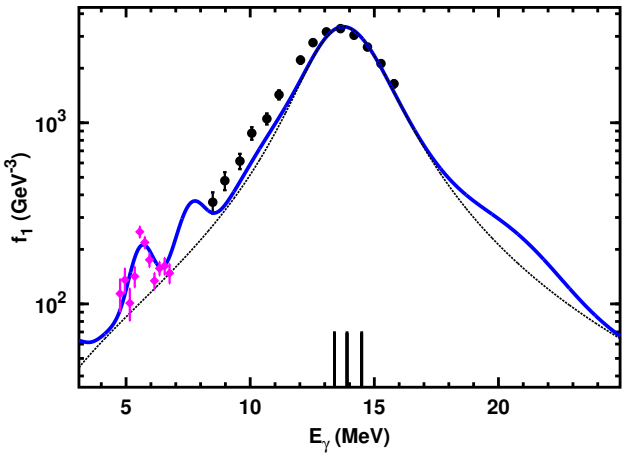

FIG. 17. (Color online) Photon strength in ^{202}Hg calculated by TLO for the IVGDR (see the caption of Fig. 7) is compared to photon scattering (magenta diamonds [94]) and photoneutron production (black circles [152]), respectively, both studied with ^{nat}Hg.

up to the IVGDR range, related to the large shell correction in near-magic nuclei; the averaging by rebinning in our figures helps to see the smooth features. Indications of contributions from the GQR are observed as well; unfortunately related electron scattering data [53, 158, 159] do not allow a fully consistent transfer of information. Inelastic proton scattering [160] indicates a peak at 21.5 MeV which could be either IVGQR or IVGMR, whereas the ISGQR is indicated in figs. 12 to 18 to partly overlap the low energy slope of the IVGDR component with the smallest E_i. In nuclei with or near closed shells the calculations predict more deformation [69] as deduced from B(E2)-values and, as found within the study presented here, in disaccord to the deformation induced splitting of the IVGDR. For closed shell nuclei a small deformation (reduced by a factor 0.4 to 1 as discussed together with Fig. 5) results in a better description of the IVGDR peak shape; this reduction has no significant influence on the strength in the tail region. In Figs. 19 and 20 three sets of experimental data for ^{232}Th and ^{238}U, respectively, in the range of the IVGDR are displayed together: The data with the large error bars were obtained by photon absorption with subsequent subtraction of the dominating atomic absorption, which had to be determined by a precise calculation. They agree within uncertainty to data stemming from a photo-neutron experiment performed at Saclay, which were reduced here by 10%, as explained before. The agreement is not perfect, but indicates the reliability of both in the IVGDR regime. The agreement between two data sets is important with respect to the disagreeing data obtained at Livermore [161]. These cross sections for ^{232}Th and ^{238}U are exceptional large in the sense, that an analysis on the basis of Eq. (10) indicates an overshoot of $\approx$ 30% as compared to

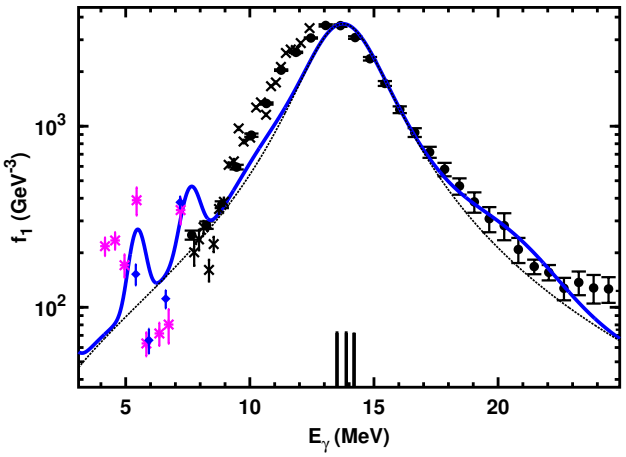

FIG. 18. (Color online) Photon strength for ^{208}Pb derived from photon scattering data using a quasi-monochromatic beam [94](blue diamonds), from bremsstrahlung [131](magenta star symbols) and from two photoneutron cross section measurements [152] (black circles), [155] (black x). TLO for the IVGDR is depicted as described for Fig. 7

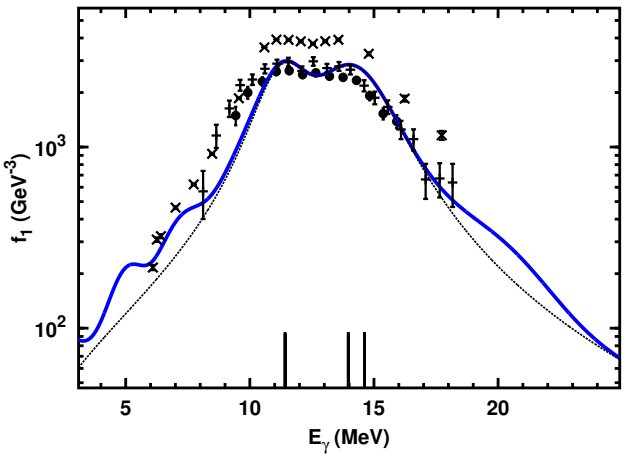

FIG. 19. (Color online) Photon strength for ^{232}Th derived from photoneutron production cross sections from Saclay [152](black circles) and from Livermore [161](black x symbols); both include photofission. Photon absorption data (black + symbols) [162] disagree to the latter, but agree to TLO (see the caption of Fig. 7)

.

the TRK sum. Low energy strength observed in actinide nuclei [164] suffers from the missing parity assignment; a questionable choice for the IVGDR tail is likely to be have influenced. Some difference of these data as compared to previous e- and γ-scattering [165] is indicated, and these assign the multipole character as M1.

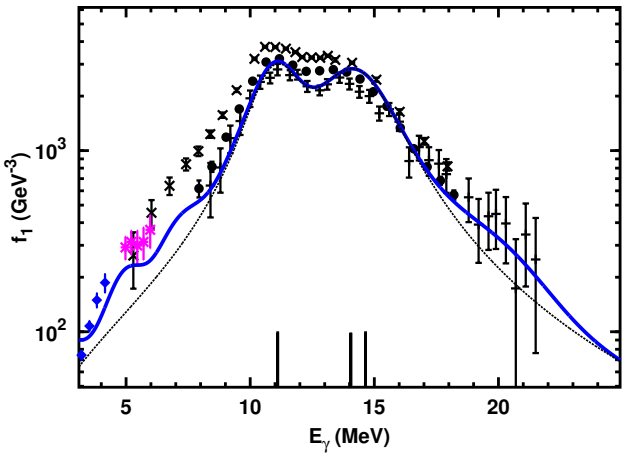

FIG. 20. (Color online) Photon strength for ^{238}U predicted by from TLO for the IVGDR (see the caption of Fig. 7) in comparison to two differing sets of data derived from the cross section of photo-neutron production ([152]black dots)([161]black x symbols); both include photofission. Also shown are photon absorption results ([162]black + symbols with large error bars) and data from photon scattering ([163]magenta *-symbols) using a quasi-monochromatic beam. Data from γ-decay after deuteron-scattering [164] at energies below 4 MeV are depicted as blue diamonds.

Odd nuclei

The CHFB calculations [5] on which our TLO parameterization is based have not yet been published for odd nuclei. As proposed [166], we use an average over the axis lengths for even neighbor nuclei to obtain f_{E1} from Eqs. ((11, 12 and 13)). It was also assumed, that for $J_0 \neq 0$ photon absorption into a mode λ populates m members of a multiplet with m=min(2λ+1, 2J_0+1) and the decay widths to the ground state Γ_{0r} are equal for each member of the multiplet; the conditions for the validity of Eq. (13) are thus fulfilled. The strength observed corresponds to the cross section summed over the multiplet and this can be described by an effective g, which according to Eq. (9) is:

$$g_{eff} = \sum_{r=1,m} \frac{2J_r+1}{2J_0+1} = 2\lambda + 1 \qquad (15)$$

This ansatz is valid in heavy nuclei [16] as it relates to the condition of weak coupling between the odd particle and the mode λ. The TLO-calculations for odd-A nuclei as shown in figs. 21 to 23 were performed on the basis of Eqs.(11, 12 and 13) with $k = 3$. No extra spin dependent factors are needed and agreement to the experimental data is found to be similar as for even nuclei, also in the tail region below S_n. In Fig. 21 data for ^{127}I are shown to be close to those for neighbouring even nuclei depicted in Figs. 11 and 12. The agreement to TLO is obvious and also "minor" pygmy strength and the IVGQR are seen.

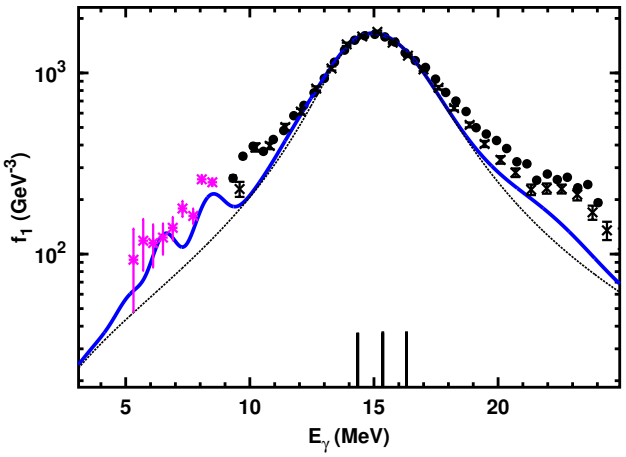

FIG. 21. (Color online)Photon strength for ^{127}I calculated as described in the text (see the caption of Fig. 7), in comparison to two datasets of photoneutron production shown as black x-symbols [116] and black points [147](reduced by 10% like all data from Saclay; this factor reduces the disagreement to the other, newer measurement). The photo-absorption data below S_n (magenta asterisk) are derived from elastic scattering by the neighbour nucleus ^{128}Xe [96], E1 and M1 added and modified by 0.7.

For the nucleus ^{197}Au not only the TLO-prediction is

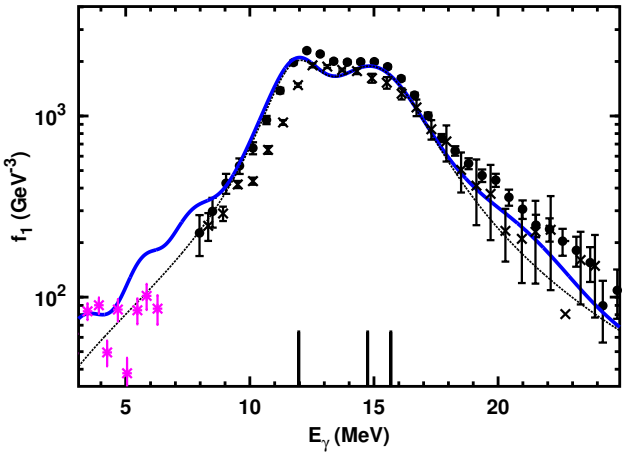

FIG. 22. (Color online) Photon strength derived for ^{181}Ta from photon scattering [96](magenta *-symbols, below 7 MeV, modified by 0.7) and from photoneutron production (black x symbols, [167]; black dots, [147]) in comparison to TLO (see the caption of Fig. 7).

depicted, but also a SLO curve from RIPL-3 [55, 56], which clearly over-predicts the data below S_n extracted from Fig. 18 of ref. [16]. In contrast to the missing strength as compared to a single Lorentzian used there, the agreement is reasonable for TLO, as the discontinuity near 19 MeV may be related to the known [119] incorrect separation of the 2n-channel. The inclusion of triaxiality

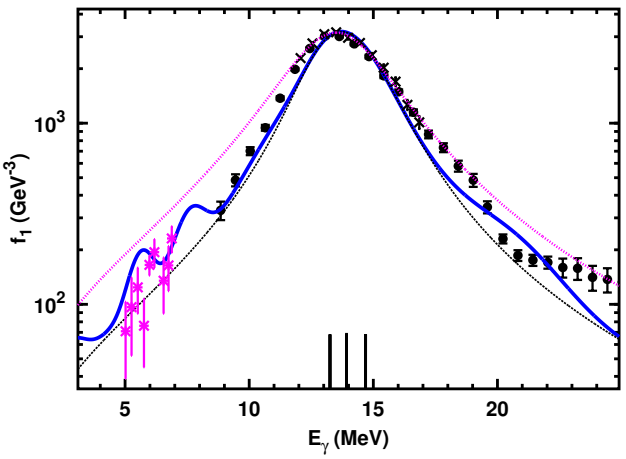

FIG. 23. (Color online) Photon strength for ^{197}Au derived from photon scattering data [16](magenta asterisks) using a quasi-monochromatic beam and from the cross section of photoneutron production [152](black circles) in comparison to the TLO prediction (see the caption of Fig. 7). Also shown are newer data for the peak region [116](black x- symbols) and a SLO fit curve from RIPL-3 [56] (magenta dotted line; adjusted in height to experiment). Note that the close agreement between the two data sets is a consequence of the renormalization of the Saclay data. [152].

in TLO leads to a reduction of Γ_i and thus of σ_{abs} for sufficiently large $(E_i^2 - E_\gamma^2)^2$ in Eq. (11). The widths Γ_i used previously [16] are 2.9 and 4.0 MeV and an additional factor of 1.22 was obtained as compared to the TRK-sum rule. This factor is 1.0 for TLO and the values for Γ_i are 2.7, 3.0 and 3.5 MeV. When ^{197,198}Au are considered spherical $\Gamma \approx 4.5$ MeV results from a SLO-fit and this effects largely the strength predicted in the tail region [79, 145]; similar conclusions result from the use of the KMF-model for ^{197}Au as was proposed [79]. The satisfying agreement of TLO as presented in Fig. 23 favours our ansatz over the other models, especially when the strongly reduced number of fit parameters is regarded.

In the bombardment with photons ^{239}Pu mainly undergoes fission and the weaker neutron emission channel has to be added to obtain σ_{abs}. In Fig. 24 the result of this sum obtained in measurements at Livermore is compared to direct absorption data and a reasonable agreement is seen, as well as a good agreement to the TLO-prediction. This is remarkable in view of the disagreements depicted in Figs. 19 and 20 for the near neighbors ^{232}Th and ^{238}U and doubts about these older data seem justified. Together with the agreement between ^{88}Sr and ^{89}Y reported recently [114] the examples presented in this section support the TLO ansatz for the derivation of photon strength in odd nuclei. Hence for all nuclei presented here a quite good agreement between observations and the TLO prediction for E1 strength is found, if minor strength is accounted for at least approximately

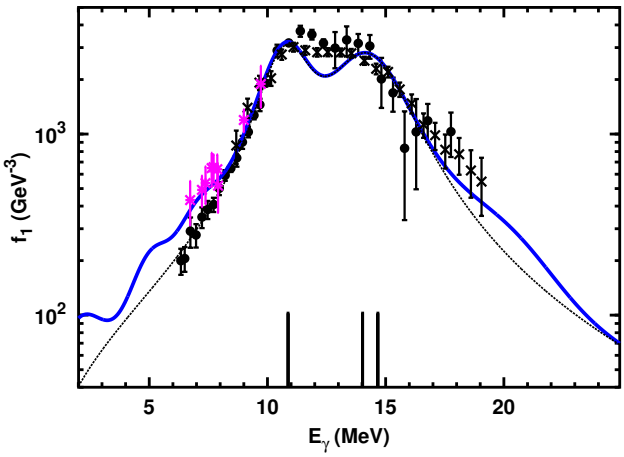

FIG. 24. (Color online) Photon strength for ^{239}Pu (black dashed curve: TLO; full blue curve: minor strength added to TLO). Data are derived from summing cross sections of fission and neutron emission induced by quasi-mono-energetic photons [168] (black circles) and by discrete γ-rays from neutron capture [169](magenta stars on the low energy slope). The absorption data from [162] (black x) were obtained with bremsstrahlung.

– for which we present a phenomenological solution. A description of the IVGDR in deformed nuclei [170] not using the TRK sum rule and not based on a fully self-consistent calculation of the shape parameters was by far less successful in its predictions.

VII. SUMMARY, COMPARISON TO OTHER WORK, AND CONCLUSIONS

The results of the comparison of experimental data for more than 20 nuclei in the mass range from 78 to 239 to Eqs.(11 and 13) can be summarized as follows:

(a) The centroid IVGDR energies derived from droplet model fits to masses [64, 171] are in accord to the data, when an effective mass $m_{eff}c^2 = 800$ MeV and the proton radii as predicted from the CHFB calculations [5] are used.

(b) Experimental data may suffer from missing exact information on detection efficiency as well as on beam resolution, eventually causing discrepancies between measurements at different laboratories – as was observed for several nuclei [116] as well as pointed out for ^{232}Th and ^{238}U.

(c) There is no indication of a strong departure from the classical dipole sum rule [13, 49] and the yield at energies above the IVGDR is assigned to the quasi-deuteron strength. Good conformance with the TRK-sum is not only observed near closed shells or for nuclei with large $|Q_0|$; previously reported [77, 78, 117] local fits together with the *ad hoc* assumption of spherical or axial symmetry overestimated IVGDR widths, resulting in the excess over TRK.

(d) The IVGDR data together with data for high as well as for lower energies do not allow for a strong variation of the width with photon energy, as previously postulated [52]; in respective data analysis higher width values [56, 77, 78] compensated such a decrease at low energy, but this caused a too large strength there.

(e) The resonance widths vary only smoothly with A and Z and depend on the resonance energies via a power law (*cf.* Eq. (12)), predicted by hydro-dynamical considerations [60, 68, 157, 172]. Only by allowing broken axial symmetry, three rather narrow resonance parts add up to an IVGDR structure with an apparent width as large as observed; this indicates the importance of extra information on shapes [14] as*e.g.* coming from CHFB calculations [5].

(f) Having Γ depend on E_i only, (12) causes the two upper Lorentzians (and their sum) in nuclei with large Q_0 (see figs. 13, 14, 19, 20, 22 and 24 to have reduced height albeit all three components have equal strength.

(g) If an enhancement by intermediate structures is handled as minor strength similar to previous work for nearly magic nuclei [15, 94] also the lower energy dipole strength in nuclei of intermediate deformation (figs. 11, 12, 15, 16, 21 and 23) is reasonably well accounted for in TLO (plus 'minor' strength, cf. Table I) – with a much lower number of parameters in comparison to previous work [59, 79, 115].

(h) In γ-decay spectra observed after average n-capture (ARC) as well as in photon scattering two E1 pygmy modes are seen in nuclei with $A > 70$ (if the respective energy range is covered); both kind of data are in reasonable accord to each other.

(i) For lower energies the scissors M1 mode was predicted [18] to also be a general feature in heavy nuclei, but in photon scattering a clear separation from the E1 strength originating from quadrupole-octupole coupling is needed.

(j) The higher pygmy photon strength may well be due to an isoscalar vortical proton motion [97, 150]. A vibration of excess neutrons against a core, was predicted [173] to appear below $\approx 0.4E_{IVGR}$ and to cause excess above the Lorentzian tail; but in this energy range E1 strength may as well be related to neutron p-h modes, which were shown [72, 174]to be strong in ^{208}Pb.

(k) Exact deformation parameters are unimportant for the tail of the E1-resonance and thus also for the photon strength, which is of importance to neutron capture processes. Experimental data below S_n used as an argument for parameterizations other than TLO [79, 175] can well be described by TLO, if the extra 'minor' strength is added (cf. Figs. , 13 to 16).

(l) An account for the variance of the deformation parameters by instantaneous shape sampling [85] only leads to small changes of the calculated strength in the IVGDR for deformed nuclei: The resonances are widened near the peak region, but the low energy tail remains unchanged.

(m) As discussed in our earlier work [14, 66] TLO uses small photon-energy independent damping widths depending on the resonance energies E_i only. This brings the tail down considerably, especially in the region below 7 MeV (see Figs. 12 and 23 versus Figs. 2 and 1 of [79]).

(n) The Axel-Brink hypothesis and the TRK sum rule together with the photon-energy independence of the IVGDR width are essential for our TLO-ansatz, and no clear hints for deviations are seen when comparing data to TLO.

(o) We question that an experimental proof exists for nuclear axiality in most heavy nuclei, and our work indicates a falsification of axial symmetry in the valley of stability. This resembles to what was predicted for crystalline matter by Jahn and Teller in 1937 [176, 177] and observed only much later.

Most of the points listed above are directly related to our proposal to not assume *ad hoc* axial symmetry for nuclei in the valley of stability. Admitting the breaking of axial symmetry for all heavy nuclei, albeit often weak, clearly improves a global description of Giant Dipole Resonance (IVGDR) shapes by a triple Lorentzian (TLO), introduced recently [14, 66]. Recently reviewed [55, 56] results of an analyis on the basis of local fits to optimize the agreement near the IVGDR peak are depicted in Fig. 25. Its lower part shows the missing agreement of such fits with the TRK sum; the large unsystematic scatter obtained in these local fits speaks againts against their use *e.g.* for nuclear astrophysics, but it has been proposed [178] to be used in that field. The upper panel of Fig. 25 shows how the pole energies and Lorentz widths from the local fits as published within RIPL-3 [55, 56] scatter as compared to the description of the IVGDR shapes, allowing three poles and thus a 'triple' Lorentzian (TLO) parameterization, derived from the global fit procedure detailed in section IV. As seen from Fig. 25 the TLO-method results in a smooth dependence on A which is modulated only due to variations in shape, as presented in sections IV and VI. As shown in the bottom part of Fig. 25, the TRK sum rule, Eq. (10), disagrees in many nuclei to the Lorentzian fits [56, 78] performed for the

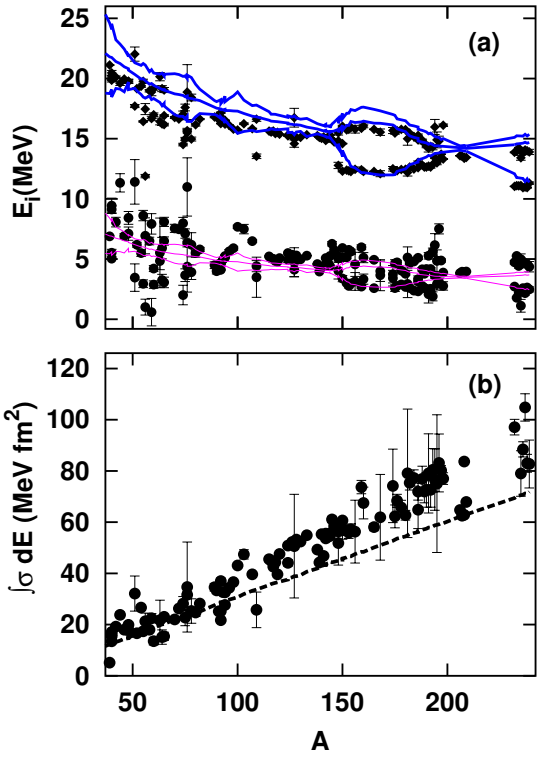

FIG. 25. (Color online) Panel (a) shows the energies (top) and widths (bottom, both vs. mass number) resulting from χ^2-fits to the IVGDR in heavy nuclei, as compiled recently [56]. The fits are based on one or two Lorentzians and two points per nucleus are shown, if a 2-pole fit led to a smaller χ^2. Our calculations with 3 poles (TLO) as described in section IV are depicted as three drawn curves for the three components of the IVGDR's; (blue for E_i and magenta for Γ_i). In panel (b) the resulting GDR-integrals as obtained by the Lorentzian fits from ref. [55] are depicted in comparison to the TRK sum rule (dotted line), which is surpassed considerably in most cases, whereas TLO obeys it by definition.

data of each nucleus independently without account for the possibility of broken axial symmetry. In these fits the width parameter was adjusted for each isotope separately to fit the peak region and for A between 90 and 150 an especially large discrepancy is observed as well as wide fluctuation with Z and A of this apparent width indicating a non-systematic variation which is difficult to conceive within the spreading concept. A similarly erratic dependence of the integrated IVGDR strength on Z and A was reported [56] to result from this approach of fitting the photo-absorption data locally. In some cases the integrated cross section overshoots the classical sum rule given by Eq. (10, first term) by up to 100%. Apparently the two problems are closely related, as the resonance integral is proportional to the product of height and width.

Also recent calculations in the framework of the axially symmetric deformed quasiparticle random-phase ap-

proximation based on the finite-range Gogny force [166] do not arrive at fully convincing predictions for the strength in the IVGDR: A phenomenlogical modification was needed to avoid a strong increase of CPU-time for calculations including more and more harmonic oscillator shells. Some agreement to experimental data was obtained by adjusting both, the width and an energy shift. Here three different approaches were tested, but for none of them a clear preference was expressed. In this work it was also shown, that none of the two choices for the Gogny forces as used before by the collaboration is clearly favoured. That supports our ansatz to first describe the data phenomenologically in accord to macroscopic considerations and to leave the two globally extracted parameters m_{eff} and c_w from Eq.(12) to a future microscopic derivation. This may finally also lead to a predicition for the low energy tail eventually to be be favoured to the phenomenology proposed here. In view of its possible application to a large number of nuclides, the acount for triaxiality leads to a smooth spreading width in contrast to the interpretation of an apparent IVGDR width without any evident N or A behavior [166]. It is worth to point out that the microscopic treatments of the IVGDR in the doubly magic ^{208}Pb [67, 71, 150] as mentioned above are not hampered by eventual deformation effects. These studies do not need any fit to the experimentally observed IVGDR shapes and the width they calculate microscopically for this nucleus is in accord to the value we derive from our global fit.

The quasi identical approach as published previously [14, 66, 81–83, 86, 126, 131] and compared to data for a number of isotopes can be considered part of the present work, such that a nearly complete sample of all IVGDR data in heavy nuclei are shown to be well described by TLO. Various spectroscopic information of other kind [3, 7, 8, 29, 35, 41] indicated triaxiality for a number of heavy nuclei and we also referred to various theoretical studies on the importance of broken axial symmetry [4, 5, 7, 23, 26, 27, 31, 33, 38, 44, 65, 68, 177]. Our work may induce further studies in nuclear theory related to broken axial symmetry.

In our final conclusion we stress three points connected to broken axial symmetry:

1. *Ad hoc* assumptions on shapes should be replaced by information from outside like the direct prediction of triaxiality in all heavy nuclei as derived theoretically from CHFB [5].

2. The triple Lorentzian (TLO) fit to IVGDR's is global in its only two free parameters – one each for energy and width, both independent of A and Z – and it allows the TRK sum rule to be fulfilled. We consider our good representation of IVGDR data for nuclei with intermediate deformation as falsification of the often assumed axiality for them, assuming which required three or more local parameters to obtain a good fit for each one nucleus [55, 56].
3. The width is not modified by an extra energy dependence and this is a consequence of the small spreading width possible in TLO. This falsification of the direct dependence of spreading width on photon energy is important for a prediction for the low and high energy tails of the dipole strength.

ACKNOWLEDGEMENTS

This work is supported by the German federal ministry for education and research BMBF (02NUK13A) and by the European Commission within the 7th EU framework programme under ERINDA (FP7-269499) and through Fission-2013-CHANDA (project no. 605203). Intense discussions within these projects and with other colleagues, especially with Ronald Schwengner, Julian Srebnry and Hermann Wolter, are gratefully acknowledged.

REFERENCES

[1] Y. Oktem et al., Phys. Rev. C 86, 054305 (2012)
[2] K. Wrzosek-Lipska et al., Phys. Rev. C 86, 064305 (2012)
[3] Y. Toh et al., Phys. Rev. C 87, 041304 (2013)
[4] T. Nikšić, P. Marević, and D. Vretenar, C 89 (2014) 044325 and refs. quoted there
[5] J.-P. Delaroche et al., Phys. Rev. C 81, 014303 (2010); ibid., supplemental material
[6] H. Schiller u. Th. Schmidt, Zeits. f. Phys. 94 (1935) 457, id., 95 (1935) 265; id., 98 (1936) 430,
[7] K. Kumar, Phys. Rev. Lett. 28, 249 (1972)
[8] D. Cline, Ann. Rev. Nucl. Part. Sci. 36, 683 (1986)
[9] K. Alder et al., Rev. Mod. Phys. 28, 432 (1956)
[10] O. Nathan and S.G. Nilsson; α, β, γ-ray spectroscopy, K. Siegbahn ed., North Holland 1965
[11] A. Bohr and B.R. Mottelson, Nucl. Phys. 4, 529 (1957); id., 9, 687 (1959)
[12] A. Bohr and B. Mottelson, Nuclear Structure ch. 6, (New York 1975)
[13] M. Gell-Mann et al., Phys. Rev. 95, 1612 (1954)
[14] A.R. Junghans et al., Phys. Lett. B 670, 200 (2008)
[15] P. Axel et al., Phys. Rev. C 2, 689 (1970)
[16] G.A. Bartholomew et al., Adv. Nucl. Phys. 7, 229 (1973)
[17] U. Kneissl et al., J. Phys. G 32, R217 (2006)
[18] K. Heyde et al., Rev. Mod. Phys. 82, 2365 (2010)
[19] E. Grosse and A.R. Junghans, Landolt-Börnstein, New Series I/25D, 4 (2012)
[20] D. Savran et al., Prog. Part. Nucl. Phys. 70, 210 (2013); id., Phys. Rev. Lett. 100, 232501 (2008)

[21] N.J. Stone, At. Data and Nucl. Data Tables 90 (2005) 75
[22] L. Esser et al., Phys. Rev. C 55, 206 (1997)
[23] J.P. Davidson, Rev. Mod. Phys. 37, 105 (1965)
[24] S. Raman et al., At. Data and Nucl. Data Tables 78, 1 (2001)
[25] J. Decharge et al. , Phys. Rev. C 21, 1568 (1980)
[26] S. Frauendorf, Rev. Mod. Phys. 73, 463 (2001)
[27] A. Hayashi, K. Hara and P. Ring, Phys. Rev. Lett. 53, 337 (1984)
[28] A. Arima and F. Iachello, Ann. Rev. of Nucl. and Part. Sc. 31, 75 (1981)
[29] J. Stachel et al., Nucl. Phys. A 419, 589 (1984); id. Nucl. Phys. A 383, 425 (1982)
[30] J. Jolie, Progress in Particle and Nuclear Physics 59, 337 (2007)
[31] F. Iachello, Phys. Rev. Lett. 91, 132502 (2003)
[32] M. Zielinska et al., Nucl. Phys. A 712, 3 (2002)
[33] A.S. Davydov and J.P. Fillipov, Nucl. Phys. A 8, 237 (1958); A.S. Davydov and V.S. Rostovsky, Nucl. Phys. 12, 58 (1969)
[34] N. Pietralla et al., Phys. Rev. Lett. 73, 2962 (1994)
[35] C.Y. Wu et al., Nucl. Phys. A 533, 359 (1991); id., Nucl. Phys. A 607, 178 (1996)
[36] C.Y. Wu and D. Cline, Phys. Rev. C 54, 2356 (1996)
[37] J. Srebnry et al., Nucl. Phys. A 766, 25 (2006); id., Int. J. of Mod. Phys. E 20, 422 (2011) and refs. quoted therein.
[38] C.A. Mallmann, Nucl. Phys. 24, 535 (1961)
[39] K. Pomorski et al. , Nucl. Phys. A 205, 433 (1973)
[40] A. Mauthofer et al., Z. Phys. A 336, 263 (1990)
[41] W. Andrejtscheff and P. Petkov, Phys. Rev. C 48, 2531 (1993); id., Phys. Lett. B 329, 1 (1994)
[42] V. Werner et al., Phys. Rev. C 71, 054314 (2005)
[43] J. Meyer-ter-Vehn, et al., Phys. Rev. Lett. 32, 383 (1974)
[44] D.L. Hill and J.A.Wheeler, Phys. Rev. 89, 1102 (1953)
[45] S.E. Larsson, Physica Scripta, 8, 17 (1973)
[46] M. Girod and B.Grammaticos, Phys. Rev. C 27, 2317 (1982)
[47] J. Levinger and H.A. Bethe, Phys. Rev. 78, 115 (1950)
[48] W. Weise, Phys. Rev. Lett. 31, 773 (1973)
[49] W. Kuhn, Zeitschr. f. Phys. 33, 408 (1925); F. Reiche and W. Thomas, Zeitschr. f. Phys. 34, 510 (1925)
[50] M.B. Chadwick et al, Phys. Rev. C 44, 814 (1991)
[51] J. Ahrens, Nucl. Phys. A, 446, 229 (1985)
[52] S.G. Kadmenskii, V.P. Markushev and V.I. Furman, Sov. J. Nucl. Phys. 37, 165 (1983)
[53] R. Pitthan et al., Phys. Rev. Lett. 33, 849 (1974); id., Phys. Rev. 21, 28 (1980)
[54] B.S. Dolbilkin et al., Phys. Rev. C 25, 2225 (1982); T. Saito et al., Phys. Rev. C 28, 652 (1983)
[55] R. Capote et al., Nucl. Data Sheets 110, 3107 (2009); id.,http://www-nds.iaea.org/RIPL-3/
[56] V.A. Plujko et al., At. Data and Nucl. Data Tables 97, 567 (2011); http://www-nds.iaea.org/RIPL-3/gamma
[57] C. Fiolhais, Annals of Physics, 171, 186 (1986)
[58] F. Bečvář et al., Phys. Rev. C 52, 1278 (1995)
[59] J. Kopecky, M. Uhl and R.E. Chrien, Phys. Rev. C 47, 312 (1993)
[60] M. Danos and W. Greiner, Phys. Rev. 134, (1964) B 284
[61] E.F. Gordon and R. Pitthan, Nucl. Inst. and Meth. 145, 569 (1977)
[62] M. Goldhaber and E. Teller, Phys. Rev. 74, 1046 (1948)
[63] H. Steinwedel and H. Jensen, Phys. Rev. 79, 1019 (1950)
[64] W.D. Myers et al., Phys. Rev. C 15, 2032 (1977)
[65] P. Möller et. al., Phys. Rev. Lett. 95, 062501 (2006); id. At. Data and Nucl. Data Tables 94 (2008) 758
[66] A.R. Junghans et al., Journ. Korean Phys. Soc. 59, 1872 (2010)
[67] C.B. Dover, R. H. Lemmer, and F. J. W. Hahne, Ann. Phys. (N.Y.) 70, 458 (1972).
[68] B. Bush and Y. Alhassid, Nucl. Phys. A 531, 27 (1991)
[69] G.F. Bertsch et al., Phys. Rev. Lett. 99, 032502 (2007)
[70] G. Enders et al., Phys. Rev. Lett. 69, 249 (1992)
[71] B. A. Brown, Phys. Rev. Lett. 85, 5300 (2000)
[72] R. Schwengner et al., Phys. Rev. C 81, 054315 (2010)
[73] R. Sedlmayr, M. Sedlmayr and W. Greiner, Nucl. Phys. A 232, 465 (1974)
[74] T.J. Bowles et al., Phys. Rev. C24, 1940 (1981)
[75] T.J. Boal, E.G. Muirhead and D.J.S. Findlay, Nucl. Phys. A 406, 257 (1983)
[76] E. Bortolani and G. Maino, Phys. Rev. C 43, 353 (1991)
[77] B.L. Berman and S.C. Fultz, Rev. Mod. Phys. 47, 713 (1975)
[78] S.S. Dietrich and B. L. Berman, At. Data and Nucl. Data Tables 38, 199 (1988)
[79] J. Kopecky and M. Uhl, Phys. Rev. C 41, 1941 (1990);
[80] H.W. Barz, I. Rotter and J. Höhn, Nucl. Phys. A 275, 111 (1977); R. Wünsch, priv. comm.
[81] R. Beyer et al., Int. J. of Mod. Phys. E 20, 431 (2011)
[82] C. Nair et al., Phys. Rev. C 81, 055806 (2010)
[83] M. Erhard et al, Phys. Rev. C 81, 034319 (2010)
[84] P. Carlos et al., Nucl. Phys. A 219, 61 (1974); id., Nucl. Phys. A 225, 171 (1974)
[85] S. Q. Zhang et al., Phys. Rev. C 80, 021307 (2009)
[86] E. Grosse et al., Eur. Ph. Journ. WoC. 21, 04003 (2012); dto., 8, 02006 (2010)
[87] G. Audit et al., Nucl. Instr. 79, 203 (1970)
[88] M. Beard et al., Phys. Rev. C 90, 034619 (2014)
[89] D. Brink, Nucl. Phys. 4, 215 (1957); dto., Ph.D. thesis, Oxford
[90] P. Axel, Phys. Rev. 126, 671 (1962)
[91] U. Kneissl et al., Progr. in Part. and Nucl. Phys. 34, 285 (1995), ibid., 37, 349 (1996)
[92] T. Kibédi and R. Spear, At. Data and Nucl. Data Tables 80, 35 (2002)
[93] L. M. Robledo and G. F. Bertsch, Phys. Rev. C 84, 054302 (2011)
[94] R.M. Laszewski and P. Axel, Phys. Rev. C 19, 342 (1979)
[95] R. Schwengner et al., Phys. Rev. C 76, 034321 (2007); id., Phys. Rev. C 78, 064314 (2008)
[96] R. Massarczyk, et al., Phys. Rev. Lett. 112, 072501 (2014)
[97] N. Ryezayeva et al., Phys. Rev. Lett. 89, 272502 (2002)
[98] T.D. Poelhekken et al., Phys. Lett. B 278, 423 (1992)
[99] J. Endres et al., Phys. Rev. C 80, 034302 (2009), id., Phys. Rev. Lett. 105 (2010), 212503
[100] R. Schwengner et al., Nucl. Phys. A 486, 43 (1988); id. Nucl. Phys. A 509, 550 (1990)
[101] R.M. Laszewski et al., Phys. Rev. Lett. 59, 431 (1987)
[102] H. Utsunomiya et al., Phys. Rev. Lett. 100, 162502 (2008)
[103] S. Goriely, E. Khan, and M. Samyn, Nucl. Phys. A739, 331 (2004)

[104] EXFOR database, e.g. https://www-nds.iaea.org/exfor/exfor.htm
[105] A. Sonzogni, (2012); www.nndc.bnl.gov/nudat2/indx_adopted.jsp
[106] Yu.P. Popov et al., Nucl. Phys. A 188, 212 (1972); id., Sovj. Journ. of Part. and Nuclei, 13, 483 (1982)
[107] L. Aldea et al., Z. Physik A 283, 391 (1977)
[108] W. Furman et al., Phys. Lett. B 44, 465 (1973)
[109] R. Schwengner, S. Frauendorf, and A. Larsen, Phys. Rev. Lett. 111, 232504 (2013)
[110] H.R. Weller and N.R. Roberson, Rev. Mod. Phys. 52, 699 (1980); H.R. Weller et al., Prog. in Part. and Nucl. Ph. 62, 257 (2009)
[111] G. Rusev et al., Phys. Rev. Lett. 110, 022503 (2013); id., Phys. Rev. C 87, 054603 (2013)
[112] A. van der Woude, Progr. in Part. and Nucl. Phys. 18, 217 (1987); dto. in Electr. and Magn. Giant Res., J. Speth Ed. (1991)
[113] A. Schwierczinski et al., Phys. Rev. Lett. 35, 1244 (1975)
[114] E. Grosse, A.R. Junghans and R. Massarczyk, Phys. Lett. B 739, 1 (2014)
[115] S.F. Mughabghab, C. Dunford, Phys. Lett. B 487, 155 (2000)
[116] B.L. Berman et al., Phys. Rev. C 36, 1286 (1987)
[117] H. Utsunomiya et al., Phys. Rev. C 84, 055805 (2011)
[118] V.V. Varlamov et al., J. Phys. Atom. Nucl., 67, 2107 (2004); ibid. 75, 1339 (2012)
[119] V.V. Varlamov et al., Eur. Phys. J. A 50, 114 (2014)
[120] D.J.S. Findlay, Nucl. Instr. 213, 353 (1983)
[121] P. Carlos et al., Nucl. Phys. A 172, 437 (1971)
[122] H. Beil et al.,Nucl. Phys. A 172, 426 (1971)
[123] B.S. Ishkhanov and V. V. Varlamov, Physics of Atomic Nuclei 67, 1664 (2004)
[124] A. Sauerwein et al. Phys. Rev. C 89, 035803 (2014)
[125] H.T. Nyhus et al. , Phys. Rev. C 91, 015808 (2015)
[126] C. Nair et al., Phys. Rev. C 78, 055802 (2008)
[127] A.P. Tonchev et al., Phys. Rev. Lett. 104, 072501 (2010)
[128] A. Jung et al., Nucl. Phys. A 584, 103 (1995)
[129] K. Govaert et al., Phys. Rev. C 57, 2229 (1998)
[130] G. Rusev et al., Phys. Rev. C 77, 064321 (2008); id., Phys. Rev. C 79, 061302 (2009)
[131] G. Schramm et al., Phys. Rev. C 85, 014311 (2012)
[132] R. Massarczyk, et al., Phys. Rev. C 86, 014319 (2012)
[133] P. Carlos et al., Nucl. Phys. A 258, 365 (1976)
[134] G. Rusev et al., AIP Conf. Proc. 1099, 799 (2009); http://link.aip.org/link/doi/10.1063/1.3120158
[135] M. Guttormsen et al., Phys. Rev. C 71, 044307 (2005)
[136] A.C. Larsen and S. Goriely, Phys. Rev. C 82, 014318 (2010)
[137] H. Beil et al., Nucl. Phys. A 219, 61 (1974); id., Nucl. Phys. A 227, 427 (1974)
[138] A. Leprêtre et al., Nucl. Phys. A 219, 39 (1974)
[139] B. Oezel-Tashenov et al., Phys. Rev. C 90, 024304 (2014)
[140] H.K. Toft et al., Phys. Rev. C 83, 044320 (2011) ; id., Phys. Rev. C 81, 064311 (2010)
[141] J. Isaak et al., Phys. Lett. B 727, 361 (2013)
[142] A. Koning et al., Nucl. Phys. A 810, 13 (2008); dto., http:\www.talys.eu
[143] T. von Egidy and D. Bucurescu, Phys. Rev. C 80, 054310 (2009)
[144] M. Krticka et al., Phys. Rev. Lett. 92, 172501 (2004); dto., J. Phys. G. 35, 014025 (2008)
[145] G.M. Gurevich et al., Nucl. Phys. A 351, 257 (1981)
[146] O.V. Vasilyev et al., Sovj. Journ. Nucl. Phys.,13, 259 (1969); id., Yadernaja Fizika 13,463 (1971)
[147] H. Bergére et al., Nucl. Phys. A 121, 463 (1968); id., Nucl. Phys. A133, 417 (1969)
[148] R. Casten et al., Nucl. Phys. A 316, 61 (1979)
[149] B.L. Berman, et al., Phys. Rev. C 19, 1205 (1979)
[150] A. Repko et al. , Phys. Rev. C 87, 024305 (2013)
[151] A.M. Goryachev and G.N. Zalesnyy; Sov. J. Nucl. Phys. 27, 779 (1978), from Yad. Fiz. 27, 1479 (1978)
[152] A. Veyssiere et al., Nucl. Phys. A159, 561 (1970); ibid, A 199,45 (1973); id., Journal de Physique 36, L267 (1975),
[153] N. Pietralla et al., Phys. Lett. B, 134 (2009)
[154] A. Zilges et al., Progr. in Part. and Nucl. Phys. 55, 408 (2005), id., AIP Conference Proceedings 831, 147 (2006)
[155] R. Van de Vyver et al., Zeitschr. f. Phys. A 284, 91 (1978)
[156] Z.W. Bell et al., Phys. Rev. C 25, 791 (1982)
[157] A.M. Nathan, Phys. Rev. C 43, 2479 (1991)
[158] F. R. Buskirk et al., Phys. Lett. B 42, 194 (1972)
[159] G. Kühner et al., Phys. Lett. B104, 189 (1981)
[160] C. Djalali et al., Nucl. Phys. A 380, 42 (1982)
[161] J.T. Caldwell et al., Phys. Rev. C 21, 1215 (1980)
[162] G.M. Gurevich et al., Nucl. Phys. A 273, 326 (1976)
[163] Y. Birenbaum, et al., Phys. Rev. C 36, 1293 (1987)
[164] M. Guttormsen et al., Phys. Rev. C 89, 014302 (2014)
[165] R.D. Heil et. al., Nucl. Phys. A 476, 39 (1988)
[166] M. Martini et al. , Phys. Rev. C 94, 014304 (2016)
[167] R. Bramblett et al.,Phys. Rev. 129 2723 (1963)
[168] B.L. Berman et al., Phys. Rev. C 34, 2201 (1986)
[169] M. Antonio, P.V. de Moraes, and M.F. Cesar, Physica Scripta 47, 519 (1993)
[170] J.A. Maruhn et al., Phys. Rev. C 71, 064328 (2005)
[171] P. Möller et. al., At. Data and Nucl. Data Tables 59, 185 (1995)
[172] M. Danos, Nucl. Phys. 5, 23 (1958)
[173] R. Mohan, M. Danos and L. C. Biedenharn, Phys. Rev. C 3, 1740 (1971)
[174] A. Heusler et al., Phys. Rev. C 89, 024322 (2014)
[175] S.F. Mughabghab, C. Dunford, Phys. Rev. Lett. 81, 4083 (1998)
[176] H.A. Jahn and E. Teller, Proc. Roy. Soc. A161, 220 (1937)
[177] P.G. Reinhard and E.W. Otten , Nucl. Phys. A 420, 173 (1984)
[178] S. Goriely, Phys. Lett. B 436, 10 (1998)